

Synthesis and Structure–Activity Relationships for 2,4-Dinitrobenzamide-5-mustards as Prodrugs for the *Escherichia coli nfsB* Nitroreductase in Gene Therapy

Graham J. Atwell, Shangjin Yang, Frederik B. Pruijn, Susan M. Pullen, Alison Hogg, Adam V. Patterson, William R. Wilson, and William A. Denny*

Auckland Cancer Society Research Centre, School of Medical Sciences, The University of Auckland, Private Bag 92019, Auckland 1142, New Zealand

Received September 7, 2006

A series of 2,4-dinitrobenzamide mustards were prepared from 5-chloro-2,4-dinitrobenzoic acid or the corresponding 5-dimesylate mustard as potential prodrugs for gene-directed enzyme prodrug therapy (GDEPT) with the *E. coli nfsB* nitroreductase (NTR). The compounds, including 32 new examples, were evaluated in four pairs of NTR^{+ve/-ve} cell lines for selective cytotoxicity (IC₅₀ and IC₅₀ ratios), in multicellular layer (MCL) cultures for bystander effects, and for in vivo activity against tumors grown from stably NTR transfected EMT6 and WiDr cells in nude mice. Multivariate regression analysis of the IC₅₀ results was undertaken using a partial least-squares projection to latent structures model. In NTR^{-ve} lines, cytotoxicity correlated positively with logP, negatively with hydrogen bond acceptors (HA) and donors (HD) in the amide side chain, and positively with the reactivity of the less-reactive leaving group of the mustard function, likely reflecting toxicity due to DNA monoadducts. Potency and selectivity for NTR^{+ve} lines was increased by logP and HD, decreased by HA, and was positively correlated with the leaving group efficiency of the more-reactive group, likely reflecting DNA crosslinking. NTR selectivity was greatest for asymmetric chloro/mesylate and bromo/mesylate mustards. Bystander effects in the MCL assay also correlated positively with logP and negatively with leaving group reactivity, presumably reflecting the transcellular diffusion/reaction properties of the activated metabolites. A total of 18 of 22 mustards showed equal or greater bystander efficiencies in MCLs than the aziridinylbenzamide CB 1954, which is currently in clinical trial for NTR-GDEPT. The dibromo and bromomesylate mustards were surprisingly well tolerated in mice. High MTD/IC₅₀ (NTR^{+ve}) ratios translated into curative activity of several compounds against NTR^{+ve} tumors. A bromomesylate mustard showed superior activity against WiDr tumors grown from 1:9 mixtures of NTR^{+ve} and NTR^{-ve} cells, indicating a strong bystander effect in vivo.

Introduction

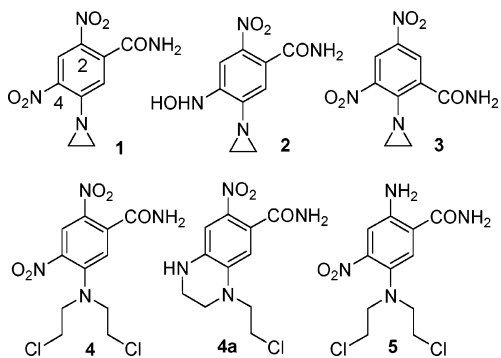
Nitroaromatic compounds are an attractive motif as prodrugs for gene-directed enzyme prodrug therapy (GDEPT) in conjunction with nitroreductase (NTR) enzymes, because there is a very large difference in electronic properties induced by the reduction of an aromatic nitro group ($\sigma_p +0.78$) to the corresponding hydroxylamine ($\sigma_p -0.32$) or amine ($\sigma_p -0.66$). This large change provides a robust “electronic switch” for prodrug activation.^{1,2} The NTR most widely explored for GDEPT purposes is the product of the *E. coli nfsB* gene, which codes for an oxygen-insensitive NTR.³ NTR reduces a range of nitro compounds to the corresponding hydroxylamines, including the prodrug 5-aziridinyl-2,4-dinitrobenzamide **1** (CB 1954).^{4,5} The latter is reduced by NTR to an equal mixture of the 2- and 4-hydroxylamines, and the 4-hydroxylamine (**2**) is then further activated by formation of *N*-acetoxy derivatives to form a DNA interstrand crosslinking agent.⁶ This was originally considered to be the major cytotoxic metabolite from **1**. However, recent studies demonstrate that the corresponding 2- and 4-amines are the major end metabolites in tumor cells and suggest that the cytotoxic 2-amino metabolite may be the main mediator of “bystander” effects (killing of adjoining non-NTR-expressing cells via local diffusion of active metabolites).⁷ Bystander killing by **1** is an important facet of its use in GDEPT,^{7–10} because this has the potential to compensate for the nonuniform distribution of prodrug-activating enzymes delivered by gene

therapy. A phase I clinical trial of **1** has been reported,¹¹ and its combination with NTR-expressing adenovirus in GDEPT protocols is under clinical evaluation.⁵

The ability of the NTR metabolites of **1** to provide a bystander effect and their activity against noncycling tumor cells¹² makes this an attractive GDEPT prodrug. However, **1** has some significant liabilities, including low aqueous solubility and low plasma AUC values achievable in humans.¹¹ The reported dose-limiting toxicities in humans are gastrointestinal and hepatic,¹¹ the latter possibly related to reduction by endogenous NTRs in human liver.¹³ In addition, the modest kinetics of the reduction of **1** by NTR¹⁴ and the limited bystander effect in 3D tumor models¹⁰ suggest room for improvement. We recently reported¹⁵ a structure–activity relationship (SAR) study of analogues of **1**, which showed the acceptability of solubilizing substituents off the carboxamide side chain. Some basic side chains provided greater selectivity than **1** for NTR^{+ve} cells, and the 2-aziridinyl-3,5-dinitrobenzamide regioisomer class (exemplified by **3**) also showed high cytotoxic selectivity in NTR-transfected cell lines, although with reduced potency. However, these aziridinylbenzamide analogues generally showed weaker bystander effects than **1** in vitro and inferior therapeutic activity to **1** against NTR-expressing tumors.

Earlier work showed that replacement of the aziridine unit of **1** with a mustard group was also acceptable for reductive activation by NTR. In fact, the corresponding chloromustard **4** (SN 23862), originally studied as a hypoxia-activated prodrug,¹⁶ was superior to **1** as an NTR substrate, with a 4-fold higher k_{cat} for purified enzyme¹⁷ and 2–3-fold faster reduction by NTR-

* To whom correspondence should be addressed. Tel.: 64 9-3737-599 x86144. Fax: 64 9-3737-502. E-mail: b.denny@auckland.ac.nz.



expressing mammalian cells.⁷ Although the 4-nitro group is the more electron affinic of the two in mustard **4**, as demonstrated by its preferential reduction by radiolysis,¹⁸ NTR reduces this compound exclusively at the 2-position to give the corresponding 2-hydroxylamine,¹⁷ with the electron release to the mustard activating it directly to a cytotoxic DNA crosslinking species.¹⁹ The reduction of only the 2-nitro group of **4** is consistent with the crystal structures of **1** and **4** complexed to the reduced enzyme.²⁰ The aziridine unit in **1** is sufficiently small that the prodrug can bind in one of the active sites of the homodimeric enzyme with the 2-nitro stacked above the FMN and, in the other active site, in an alternative orientation where only the 4-nitro group can gain access to the prosthetic group. In contrast, the more bulky mustard in **4** limits the binding orientation in both sites to the one in which only the 2-nitro group can stack above the FMN. In NTR-expressing cells, the 2-amine (**5**) rather than the 2-hydroxylamine is the dominant bystander metabolite from **4**, as demonstrated by bioassay of extracellular medium and is a more potent cytotoxin than the reduction products of **1**.⁷ The latter study also showed that **5** has superior tissue diffusion properties to the reduced metabolites of **1**, consistent with earlier studies demonstrating that **4** provides a more efficient NTR bystander effect than **1** in multicellular layer (MCL) cultures.¹⁰

For these reasons, we were interested in extending SAR for the 2,4-dinitrobenzamide mustard class of NTR prodrugs, exemplified by **4**, as potential prodrugs for activation by *E. coli* NTR. An earlier study²¹ of a small series of 2,4-dinitrobenzamide mustards in a V79 chinese hamster fibroblast cell line expressing NTR showed that the dibromo- and diiodocarboxamides (**23**, **31**) had higher potencies than **1** toward NTR-expressing cells, but that carboxamide substitution (with 2,3-dihydroxypropyl; e.g., compound **33**) was not favorable. In the present study, we extend both the range of analogues studied and the panel of NTR-expressing cell lines to explore further the SAR between activity and both side chain and leaving group substitution. In addition, we compare bystander efficiency of the 2,4-dinitrobenzamide mustards in tissue culture models and tumors in mice.

Chemistry

Compounds **4**, **8**, **11**, **14–16**, **21**, **23**, **31**, **33**, **34**, **36**, and **47** have been reported previously and were prepared by the methods reported in the references listed in Table 1. Other variants were prepared by the routes outlined in Schemes 1–5. Most involved conversion of the chloro- or bromo-mustard acids (**54**, **55**) to the corresponding acid chlorides, followed by reaction with the appropriate amines (Scheme 1). The mustards **28** and **30** were prepared from 5-chloro-2,4-dinitrobenzoic acid (**56**) by initial construction of the carboxamide side chain and subsequent formation of the mustard group (Scheme 2), while the dimesyl-

ate (**35**), bromomesylates (**41**, **42**) and diiodomustard (**32**) were prepared from the dimesylate acid (**52**) (Scheme 3). The asymmetric mustards **38**, **39** and **43** were formed via selective mesylate replacement by halogen using lithium or sodium halides (Scheme 4). Finally, the methylsulfonyl analogues **45**, **46** and **48** were prepared by broadly similar methods from appropriate 2- or 4-methylsulfonyl starting materials **62** and **65**, respectively (Scheme 5).

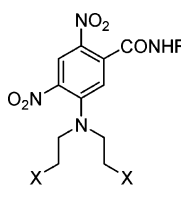
Results and Discussion

Solubility, Stability, and Lipophilicity. The solubilities and stabilities of the compounds (in culture medium with 5% fetal calf serum) were determined by HPLC. LogP values (*n*-octanol/water) were measured as described previously²² and used to train the program ACD/LogP v9.0 (Advanced Chemistry Development Labs, Inc., Ontario, Canada) using a combination of ACD/LogP System Training and Accuracy Extender. This was then used to calculate values for the other compounds. Table 1 shows that the solubility of the chloromustard **4** is enhanced (2–5-fold) by hydroxylated side chains (compounds **7** and **9–12**) and generally more substantially (from 7-fold to >65-fold) by basic or acidic side chains (compounds **13**, **14**, **17**, **20**, and **21**). We have also shown in the related aziridinybenzamide series¹⁵ the usefulness of carboxamide substitutions to increase aqueous solubility. The dibromo- and diiodomustards showed higher logP values (average 0.3 and 0.9 units, respectively) than the corresponding chloro analogues and were also less soluble. The dimesylates (**34** and **35**), despite a large decrease in logP compared with the dichloromustards (average 2.4 units), had broadly similar aqueous solubility. Likewise, the mixed mesylate/halogen mustards on average had logP values 1.4 units lower than the corresponding symmetrical halogen mustards but similar solubilities. The chloromustard prodrugs generally had good stability in culture medium (>90% remaining after 24 h at 37 °C), while the other more efficient leaving groups (bromo, iodo, mesylate) decreased stability significantly, as expected (Table 1).

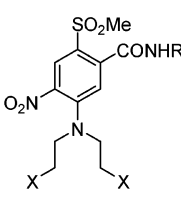
Antiproliferative Activity In Vitro. Antiproliferative potencies were evaluated by IC₅₀ assay, using 18 h drug exposures, with four pairs of cell lines; the NTR^{-ve} lines Skov3 (human ovarian carcinoma), WiDr (human colon carcinoma), V79^{puro} (chinese hamster fibroblast transfected with a control vector), and EMT6 (mouse mammary carcinoma) and the corresponding stably NTR-transfected lines Skov3-NTR^{neo}, WiDr-NTR^{neo}, V79-NTR^{puro}, and EMT6-NTR^{puro}. To simplify this large dataset, Table 1 summarizes the geometric mean values across three backgrounds (WiDr, Skov3, and EMT6), which showed very similar SAR, and for the V79 pair which also showed a similar SAR although with relatively high NTR ratios for **1** and some of the mesylate mustards (especially the dimesylate **34**). The complete set of data can be found in Table S2 in Supporting Information, which gives the means and standard errors for the IC₅₀ values in all eight cell lines, together with the ratios of the IC₅₀ values between the NTR^{-ve} and NTR^{+ve} lines.

The chloromustards **4–22** explore a wide range of side chains. Broadly, potency against NTR^{+ve} cells, and NTR selectivity, of the carboxamide **4** was retained in the analogs with mono-, di-, or trihydroxy side chains but was reduced by basic or acidic substituents. The corresponding dibromomustards **23–30** and diiodomustards **31–33** were generally more potent in the NTR^{-ve} wild-type cells, with the asymmetric halomustards **36–43** showing intermediate potencies. The dibromomustards and asymmetric bromo/chloro or bromo/mesylate mustards provided highest potency against NTR^{+ve} cells, and highest NTR ratios,

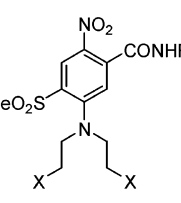
Table 1. Structures and Physicochemical Properties of Nitrobenzamide-5-mustards and Their Antiproliferative Potencies (IC₅₀ Values) against NTR^{+ve} and NTR^{-ve} Cell Lines



I



II



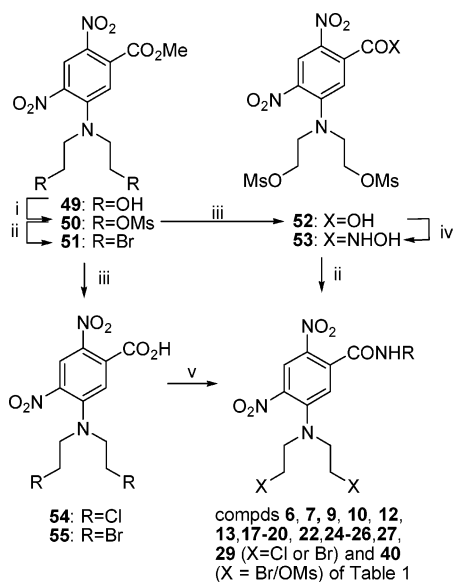
III

No	Fm	X	R	Sol ^a	Stab ^b	LogP ^c	IC ₅₀ ^d					
							V79 cells			EMT6, WiDr, and SKOV3 cells ^e		
							NTR ^{-ve}	NTR ^{+ve}	ratio ^f	NTR ^{-ve}	NTR ^{+ve}	ratio ^f
1	(CB 1954)					0.14 ± 0.00	374	0.26	2090	92	0.42	249
4^g	I	Cl	H	0.75	99	1.52 ± 0.02	490	17	42	630	5.51	133
6	I	Cl	OH	1.4	91	1.22 ± 0.03	51	1.36	42	129	1.41	91
7	I	Cl	O(CH ₂) ₂ OH	2.1	100	[2.35 ± 0.57]	750	13	76	708	12.2	58
8^h	I	Cl	(CH ₂) ₂ OH	1.0	nd	1.38 ± 0.03	312	12	59	780	4.48	179
9	I	Cl	(CH ₂) ₃ OH	4.1	108	1.49	555	7.7	77	592	4.05	153
10	I	Cl	CH ₂ CH(OH)CH ₃	1.2	107	[1.74 ± 0.23]	438	21	21	626	7.77	81
11^h	I	Cl	CH ₂ CH(OH)CH ₂ OH	2.9	100	0.93	1160	10	135	1122	4.33	275
12	I	Cl	C(CH ₂ OH) ₃	1.8	97	[1.63 ± 0.76]	1050	13	91	778	2.65	267
13	I	Cl	(CH ₂) ₂ NH ₂	9.2	99	[-0.052]	462	52	11	210	2.46	103
14^h	I	Cl	(CH ₂) ₂ NMe ₂	35	103	[1.27]	89	81	1.1	98	46.7	2.1
15^h	I	Cl	(CH ₂) ₂ N(O)Me ₂	>50	nd	[-0.64 ± 0.68]	6270	1990	3.0	5972	117	56
16^h	I	Cl	(CH ₂) ₂ Nmorpholide	5.2	100	1.60	201	130	1.6	282	71.6	4.2
17	I	Cl	(CH ₂) ₃ Nmorpholide	22	96	[0.38]	348	105	3.4	282	49.2	6.0
18	I	Cl	(CH ₂) ₄ Nmorpholide	2.0	91	[0.25]	142	25	5.9	180	11.7	17
19	I	Cl	(CH ₂) ₂ Nimidazolide	0.5	94	[0.95]	273	46	6.6	233	4.89	51
20	I	Cl	(CH ₂) ₃ Nimidazolide	19	70	[1.79]	174	32	7.4	211	31.1	15
21^h	I	Cl	(CH ₂) ₂ CO ₂ H	11	nd	[-1.48]	4890	470	9.5	5531	790	7.9
22	I	Cl	SO ₂ Me	17	100	[-0.49]	328	237	1.5	850	215	4.2
23^g	I	Br	H	0.04	98	1.97	43	0.18	302	48	0.14	344
24	I	Br	OH	1.2	69	[1.24]	34	0.2	180	44	0.20	202
25	I	Br	(CH ₂) ₂ OH	0.32	76	1.69 ± 0.01	80	0.43	203	70	0.20	350
26	I	Br	(CH ₂) ₃ OH	0.17	83	1.81 ± 0.01	37	0.28	135	64	0.14	483
27	I	Br	CH ₂ CH(OH)CH ₂ OH	1.7	102	1.25	275	0.34	828	184	0.24	819
28	I	Br	(CH ₂) ₂ CO ₂ Me	0.28	70	[2.38 ± 0.89]	52	1.1	45	87	1.42	70
29	I	Br	(CH ₂) ₃ Nmorpholide	0.86	74	[0.76]	54	13	4.5	48	5.18	9.9
30	I	Br	(CH ₂) ₂ CO ₂ H	8.4	nd	[-1.10]	148	16	9.2	127	31.4	4.0
31^g	I	I	H	0.04	69	2.41	11	0.2	54	22	0.22	106
32	I	I	(CH ₂) ₂ OH	0.4	23	[2.41 ± 0.21]	nd	nd	nd	28	0.88	32
33^g	I	I	CH ₂ CH(OH)CH ₂ OH	0.96	90	1.79	114	1.0	100	71	0.38	195
34^g	I	OMs	H	0.53	nd	-0.70	536	0.49	1200	101	0.64	209
35	I	OMs	CH ₂ CH(OH)CH ₂ OH	9.0	54	[-1.70 ± 0.63]	237	16	13	321	12.3	28
36^h	I	Cl/OMs	H	0.84	nd	0.42 ± 0.02	504	0.55	1060	300	0.55	662
37	I	Cl/OMs	CH ₂ CH(OH)CH ₂ OH	2.1	74	[-0.52 ± 0.24]	nd	nd	nd	1271	4.85	318
38	I	Cl/Br	H	0.63	62	1.61 ± 0.05	139	0.59	237	172	0.39	525
39	I	Br/OMs	H	0.23	71	0.49 ± 0.02	133	0.11	1260	94	0.13	748
40	I	Br/OMs	OH	1.5	48	[-0.20]	97	0.9	112	101	0.88	121
41	I	Br/OMs	(CH ₂) ₂ OH	1.7	70	0.46 ± 0.02	633	1.0	620	230	0.46	537
42	I	Br/OMs	CH ₂ CH(OH)CH ₂ OH	1.3	63	-0.05 ± 0.00	733	1.0	1660	860	2.01	451
43	I	I/OMs	H	0.20	72	0.74 ± 0.02	101	0.29	311	81	0.28	310
44	I	OSO ₂ NH ₂	H	1.8	95	-0.95 ± 0.05	650	0.87	788	663	2.3	309
45	II	Cl	H	0.06	74	[0.01 ± 0.38]	>50	>50	nd	>50	>50	nd
46	II	Cl	CH ₂ CH(OH)CH ₂ OH	16	106	[0.93 ± 0.40]	843	427	2.3	1767	519	3.5
47ⁱ	III	Cl	H	0.33	nd	[1.02 ± 0.77] ^j	767	9.5	73	511	11.5	46
48	III	Br	H	0.07	63	1.18 ± 0.00	80	0.16	508	50	0.28	213

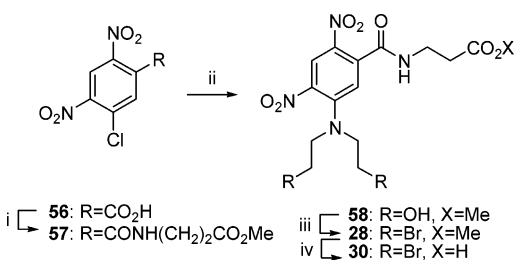
^a Solubility (mM) in α -MEM with 5% fetal calf serum, at ambient temperature, measured by HPLC. ^b % parent compound remaining, under the conditions of the solubility test, after holding at 37 °C for 24 h. ^c P: octanol–water partition coefficient, measured using a shake-flask method at pH 7.4 (errors are SEM). Values in square brackets are calculated at pH 7.4 using ACD/LOGP (version 9.0), trained with the measured compounds. ^d IC₅₀ (μ M) following 18 h drug exposure. See Table in Supporting Information for means and SEM for all cell lines. ^e Geometric means for WiDr, SKOV3, and EMT6 cells and their NTR transfectants. ^f Ratio = IC₅₀(NTR^{-ve})/IC₅₀(NTR^{+ve}). The value shown is the intra-experiment ratio and thus may not correspond exactly with the quotient of the two figures in the previous columns. ^g Ref 21. ^h Ref 16. ⁱ Ref 23. ^j Compound unstable; up to 30% decomposition during determination.

with many of these compounds showing greater potency and selectivity than **1** in the human cell lines. In particular, the dibromomustard **27**, Cl/OMs mustard **36**, Cl/Br mustard **38**, and Br/OMs mustards **39** and **41** have submicromolar geometric mean IC₅₀ values against NTR^{+ve} WiDr, Skov3, and EMT6 cells and mean NTR ratios of at least 500.

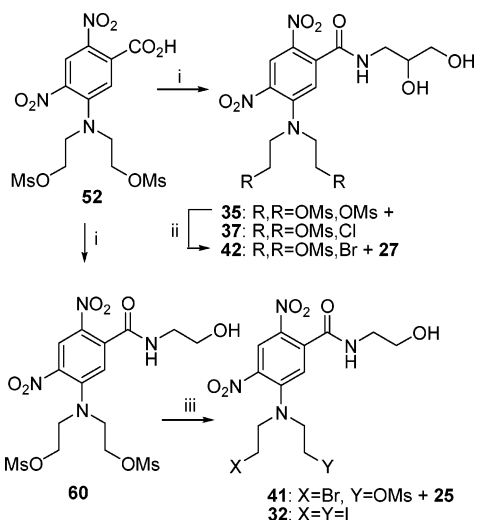
Compounds **45–48** explore the utility of replacing one of the nitro groups with the nearly equally electron-donating but more hydrophilic SO₂Me group. Metabolic studies^{7,17} have shown that reduction of the parent compound **4** by NTR occurs only at the 2-position (para to the mustard). Consistent with this, the 2-SO₂Me compounds **45** and **46** had poor potency in

Scheme 1^a

^a Reagents: (i) MsCl/Et₃N; (ii) LiBr; (iii) KOH/MeOH/dioxane/H₂O; (iv) SOCl₂/DMF, then NH₂OH; (v) SOCl₂/DMF or (COCl)₂/DMF/PhH, then RNH₂.

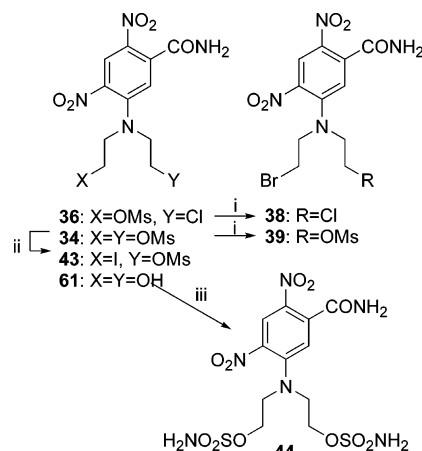
Scheme 2^a

^a Reagents: (i) SOCl₂/DMF, then NH₂(CH₂)₂CO₂Me; (ii) HN[(CH₂)₂OH]/dioxane; (iii) MsCl/Et₃N/DMF, then LiBr/EtOAc; (iv) 1 N NaOH.

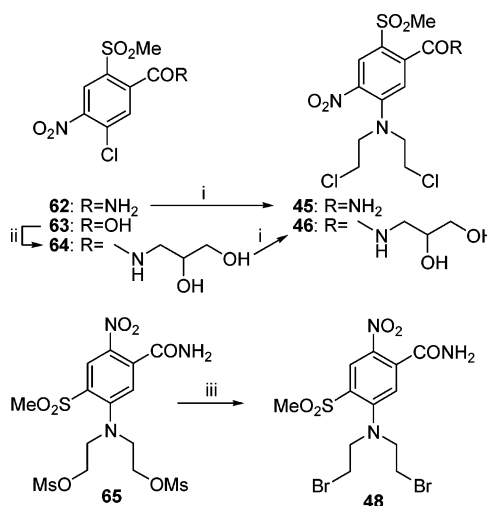
Scheme 3^a

^a Reagents: (i) SOCl₂/cat. DMF, then NH₂CH₂CH(OH)CH₂OH or NH₂(CH₂)₂OH; (ii) LiBr/EtOAc; (iii) LiBr/DMF or NaI/MeCN.

the wild-type lines and essentially no selectivity for NTR^{+ve} cells. In contrast, a previous study of the 4-SO₂Me compound **47** showed that it retained some activity in a cellular assay employing externally added NTR enzyme,²³ as well as with endogenously expressed enzyme.²¹ As expected, both **47** and its bromo analogue **48** retained potency and NTR selectivity.

Scheme 4^a

^a Reagents: (i) LiBr/MeCN; (ii) NaI/MeCN; (ii) NH₂-SO₂Cl/DMA.

Scheme 5^a

^a Reagents: (i) HN(CH₂CH₂Cl)₂/i-Pr₂NEt/dioxane; (ii) SOCl₂/DMF, then NH₂CH₂CH(OH)CH₂OH/Me₂CO/H₂O; (iii) LiBr/DMF.

Partial Least-Squares Projection to Latent Structures (PLS) Modeling of Cytotoxicity. To identify the dominant physicochemical parameters determining in vitro cytotoxicity and selectivity, QSAR of the potency and NTR ratio was undertaken on all four cell line pairs simultaneously. We used a multivariate regression approach (partial least-squares projection to latent structures; PLS), which was implemented in the SIMCA-P package. Inspection of the loading and score plots (Figure S1 and explanation of statistical parameters; see Supporting Information) confirmed that the QSAR was similar across the four cell line pairs and that simultaneous modeling was justified as illustrated for both NTR^{-ve} and NTR^{+ve} cells as well as their NTR ratios in Figure S1. The model predicted NTR ratios in the order EMT6 > Skov3 > WiDr ≈ V79 (Figure S3; Supporting Information), in reasonable agreement with measured NTR activity in these cell lines (EMT6-NTR^{puro} > Skov3-NTR^{neo} > WiDr-NTR^{neo} > V79-NTR^{puro}).¹⁵ Figure 1 shows the regression coefficients for each parameter for the PLS models describing IC₅₀ values in NTR^{-ve} (Model 1) and NTR^{+ve} cell lines (Model 2), and for their ratio (Model 3) using the cell line pair WiDr/WiDr-NTR^{neo} as example.

(a) Cytotoxicity in the Wild-Type (NTR^{-ve}) Cell Lines.

The PLS modeling identified three significant principal components (PCs) that explained 78.5% (*R*²) of the overall variability in the IC₅₀s with a cross-validated *Q*² of 57.7% (Model 1). A

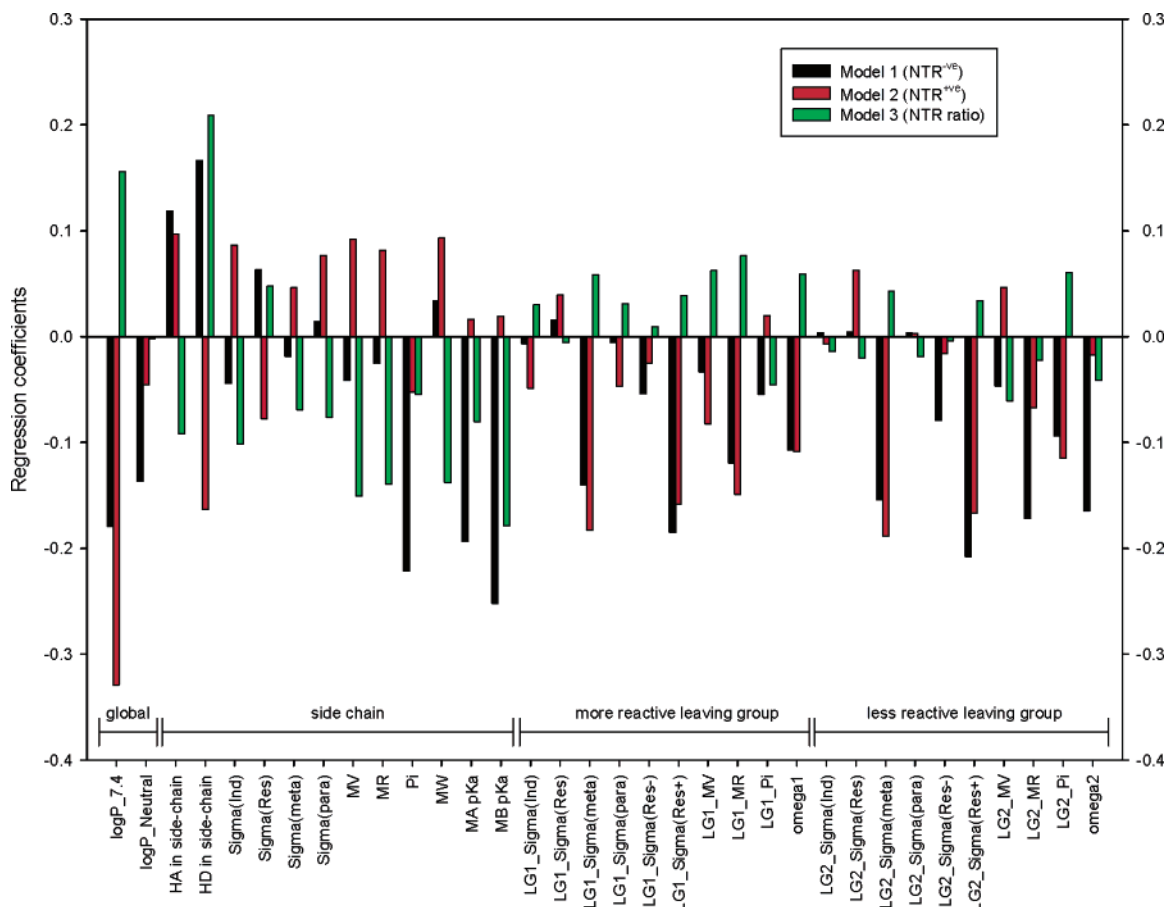


Figure 1. Regression coefficients of the physicochemical parameters (X data) in PLS Models 1, 2, and 3 used to model IC_{50} (Y data) in WiDr wild-type (NTR^{-ve} ; Model 1), WiDr- NTR^{neo} (NTR^{+ve} ; Model 2), and the ratio of IC_{50} values (Y data) in WiDr/WiDr- NTR^{neo} (NTR ratio; Model 3). The regression coefficients relate to scaled and centered X data and scaled Y data. The value of the coefficient indicates the change in the modeled Y data when the physicochemical parameter changes from 0 to 1 in standard deviations, while keeping the other parameters constant at their average value.

comparison of the model results with the experimental values are presented for the WiDr wild-type cell line (NTR^{-ve}) in Figure S2 (see Supporting Information). Missing and off-scale values for **7**, **32**, and **37** were also estimated. The regression coefficients of Model 1 are summarized in Table S3 (see Supporting Information).

As demonstrated in Figure 1, compounds with a higher overall $\log P$ were more cytotoxic with the main contribution coming from the side chain π value and minor contributions from the mustard leaving groups. Thus, the low potency of N -oxide **15** is consistent with its very low side chain π value (-3.84), whereas the very lipophilic diiodomustards (**31–33**) were the most cytotoxic. Side chain ionization (either acidic or basic) also contributed to increased cytotoxic potency, as demonstrated by the negative correlation between acidic and basic pK_a and IC_{50} (Figure 1). In contrast, side chain size and electronic property has little influence on IC_{50} , while H-bond donating or accepting groups in the side chain correlated with decreased potency.

To understand the influence of the mustard group on cytotoxicity in the parental cell lines, the two leaving groups were treated separately. The steric parameters molar volume (MV) and molar refractivity (MR) correlated positively with cytotoxic potency. The electronic parameters sigma(meta) and sigma(Res+) had a large negative effect on the IC_{50} (i.e., electron withdrawing groups increased potency), while other Hammett sigma constants did not. The correlation with sigma(Res+) is of particular significance because it points to a cationic

charge being involved. Most likely, this is the aziridinium intermediate formed during the S_N1 reaction of one of the mustard arms, with sigma(Res+) reflecting the degree of stabilization by the remaining leaving group. Cytotoxicity also correlated positively with the efficiency of the leaving group, as described by the nucleofugality parameter (ω).²⁴

For the asymmetric halomesylate mustards, the less efficient leaving group had a larger influence on cytotoxicity in the PLS model; this was consistent across all physicochemical parameters used to describe the leaving groups. A possible explanation for this is that the mustard group is activated in the NTR^{-ve} cell lines primarily by reduction of the 4-nitro group, which is the most electron-affinic.¹⁸ The resulting hydroxylamine or amine can then react intramolecularly to form the relatively nontoxic tetrahydroquinoxaline (**4a**).¹⁸ This is the major metabolite formed from **4** under both aerobic and hypoxic conditions in the human non small cell lung cancer line (A549)²⁵ and is seen in the plasma of mice treated with **4**.²⁶ The alkylating reactivity of the tetrahydroquinoxaline metabolites will be determined by the nucleofugality of the second leaving group, which is consistent with the observed QSAR in NTR^{-ve} cells. This, in turn, argues that aerobic cytotoxicity of the dinitrobenzamide mustards in aerobic tumor cells is due primarily to nitroreduction ortho to the mustard and monoalkylation of DNA, rather than DNA crosslinking or futile redox cycling leading to reactive oxygen species.

(b) Cytotoxicity in the NTR -Transfected (NTR^{+ve}) Cell Lines. PLS modeling, using the same physicochemical descrip-

tors, was also applied to the IC_{50} values obtained in the NTR^{+ve} cell lines. Compound **46** was excluded from the data set because the replacement of the 2-nitro group by the isoelectronic SO_2 -Me effectively makes this a nonsubstrate for NTR.¹⁷ Again, three significant PCs explained 79.8% (R^2) of the overall variability in the IC_{50} s with a cross-validated Q^2 of 58.5% (Model 2). A comparison of the model results with the experimental values are presented for the WiDr-NTR^{neo} cell line (NTR^{+ve}) in Figure S2 (see Supporting Information). The regression coefficients of Model 2 are summarized in Table S3 (see Supporting Information). A much stronger clustering was observed than with the wild-type lines, with the halogen mustards in one cluster, the dimesylates (**34**, **35**) and disulfamate (**44**) in another, and the mixed halomesylates (**36**, **37**, **39–43**) in a third cluster located between the first two (Figure S1). Nevertheless, because of the limited numbers in two of the three clusters, all compounds were analyzed simultaneously. As for the parental lines, the acid **21** was poorly predicted in three out of the four NTR-expressing cell lines (Skov3-NTR^{neo}, WiDr-NTR^{neo}, and EMT6-NTR^{puro}), likely due to poor cellular uptake as it showed good activation with purified NTR.¹⁷ *N*-oxide **15** was a moderate outlier in V79-NTR^{puro} cells; it is not a substrate for the purified enzyme¹⁷ and is one of the least potent mustards in all the NTR-expressing cell lines.

As in the NTR^{-ve} study, the most influential physicochemical parameter correlating positively with cytotoxicity in NTR^{+ve} cell lines was logP, with lipophilicity of both the side chain and second (less efficient) leaving group contributing (Figure 1). Ionisable side chains appeared to have little effect, in contrast to their positive contribution to potency in NTR^{-ve} cells. This is consistent with loss of sensitivity to reduction by NTR, as demonstrated for **14** and **16** with purified enzyme.¹⁷ H-bond donation properties correlated positively and H-bond accepting properties correlated negatively with potency in NTR^{+ve} cells. There was a weak tendency for compounds with larger electron-donating side chains to be less potent.

Larger leaving groups on the mustard, with larger sigma-(meta) and sigma(Res+) properties, resulted in higher potency in the NTR^{+ve} cell lines. In contrast to NTR^{-ve} cells, the nucleofugality (ω) of the first (more efficient) leaving group was more influential than the second (Figure 1). The likely reason is that the major route of activation in NTR^{+ve} cells is via reduction at the 2-nitro group, as reported for **4**,^{7,17} where there is no opportunity for internal cyclization, leaving both arms of the mustard available to form cytotoxic DNA cross-links. The 2-amine (**5**) of **4** has been reported to be much more cytotoxic than the parent compound due to its ability to form such cross-links.^{18,19}

(c) Ratios of IC_{50} Values in NTR^{+ve}/NTR^{-ve} Cell Lines (NTR Ratio). These ratios, representing the potential selectivity of the compounds as GDEPT prodrugs, were also modeled using PLS. Two approaches were followed. The first used the same approach, as described above (again excluding **46**), and resulted in two PCs that explained 70.9% (R^2) of the overall variability in the NTR ratios with a cross-validated Q^2 of 48.3% (Model 3). This is slightly less than that obtained with the PLS Models 1 and 2 for the individual IC_{50} values, likely due to the experimental noise contained in both. A comparison of the model results with the experimental values for the NTR ratio of the cell line pair WiDr/WiDr-NTR^{neo} are presented in Figure S2. The regression coefficients of Model 3 are summarized in Table S3 (see Supporting Information).

In this PLS model, four main clusters could be distinguished: one comprised compounds with basic side chains, the

neutral methylsulfonyl side chain (**22**), and halogen mustard groups; one with neutral side chains and halogen mustard groups; one with neutral side chains and mixed chloro- and bromomesylates, plus the three neutral diiodomustards; and a fourth with the mesylates (**34**, **35**), sulfamoyl analogue (**44**), and the iodomesylate **43**. The two carboxylic acids (**21**, **30**) and the aliphatic *N*-oxide (**15**) were in between the first two clusters (Figure S1). Overall, NTR ratios correlated positively with logP and side chain HD but negatively with charged side chains (especially basic ones) and HA (Figure 1). For the mustard arms, the preferred combination was a mixed chloromesylate, with selectivity favored by a hydrophilic leaving group with high ω combined with a smaller more lipophilic leaving group of lower ω . The two most potent compounds in WiDr-NTR^{neo} (**36**, **39**) were also predicted to be the most selective by Model 3; in the other three cell lines they were also among the most selective compounds.

The second approach (again excluding **46**) used a hierarchical top model based on the scores of the PLS models (base Models 1 and 2) for the parental and NTR-expressing cell lines. This also resulted in two components, which explained 76.9% (R^2) of the overall variability in the NTR ratios with a cross-validated Q^2 of 66.5%. This is a considerable improvement compared to the nonhierarchical base model (Model 3), which is most likely due to the fact that noise (e.g., experimental variation) unrelated to the respective IC_{50} values was filtered out. As expected, the results obtained with both models were similar ($R^2 = 0.911$ for WiDr/WiDr-NTR^{neo}).

Cytotoxicity and Bystander Effects in MCL Cultures. The utility of NTR prodrugs in GDEPT depends not only on their activation and cytotoxicity in NTR^{+ve} cells, but also on their ability to penetrate through the extravascular compartment and on the local diffusion of activated drug metabolites to generate a bystander effect. These requirements were evaluated using MCLs, which are a 3D cell culture model we have previously validated for measurement of bystander effects of **1** and dinitrobenzamide mustards.^{7,10,27} In these experiments, MCL co-cultures comprising 3% V79-NTR^{puro} cells (“activators”) and 97% V79^{oua} cells (NTR^{-ve} “targets” carrying a ouabain resistance gene) were exposed to prodrugs for 5 h and then dissociated with trypsin and plated in selective media to quantify clonogenic survivors from both subpopulations. From the nondrug-treated controls, the proportion of puromycin-resistant activator cells in the co-cultures averaged 2.9% (SD 1.1%) in this series of experiments. The concentration giving a surviving fraction of 10% (C_{10}) was determined for the activators and the targets in the co-cultures (A_C and T_C , respectively) and for targets grown without activators (T). These parameters are summarized for **1** and for 22 different 2,4-dinitrobenzamide-5-mustards in Table 2. All of the compounds showed high ratios of T/A_C (>10), confirming that they are good NTR prodrugs, with the exception of the morpholide **16**, which showed little differential between NTR^{+ve} and NTR^{-ve} V79 cells in 3D MCL cultures as in the IC_{50} assay.

The cytotoxic potency of the compounds against V79-NTR^{puro} cells in the MCLs showed a strong correlation with IC_{50} values against the same cell line in monolayer culture (Figure 2A). This suggests that there are no large differences in the ability of the mustards to penetrate these multicellular structures. However, it is noteworthy that the compounds with greatest potency in MCLs relative to the IC_{50} assay (i.e., that lie furthest below the regression line in Figure 2A) are the very lipophilic **4**, **31**, and **38**, while the compounds that are less potent in MCLs than expected from their IC_{50} values (**27** and **42**) have relatively

Table 2. Cytotoxicity and Bystander Effects of 2,4-Dinitrobenzamide-5-mustards in V79 MCLs^a

compd	A_C^b (μM)	T_C^c (μM)	T^d (μM)
1 ^e	23 ± 3 (3)	173 ± 27 (3)	1400 ± 180 (4)
4 ^e	98 ± 27	120 ± 20	>1000
6 ^e	43	>300	>1400
8 ^e	95 ^e	210 ^e	>1000
9 ^e	95	150	3300
11 ^e	95 ± 20	510 ± 0	3500
16 ^e	1500	3000	3500
23 ^e	3.3	4.6	>50
25 ^e	5.2	17	150
26 ^e	3	7	100
27 ^e	18 ± 4	98 ± 22	675 ± 25
31 ^e	1.65	2	>20
32 ^e	5.5	10	122
33 ^e	12.5 ± 0.5	54 ± 11	245 ± 40
34 ^e	13	152	>300
36 ^e	5.3	33	>1000
38 ^e	3.4	8.2	>300
39 ^e	2	10	>250
42 ^e	70 ± 20	>1300	>1300
43 ^e	4.2	12	>200
44 ^e	9.5	800	>1800
47 ^e	160	>300	>1000
48 ^e	5.5	16	>100

^a MCLs grown from V79^{oua} (NTR^{-ve} targets) alone, or mixtures of 3% V79-NTR^{puro} (NTR^{+ve} activators) and 97% targets, were exposed to prodrugs at a range of concentrations for 5 h under 95% O₂/5% CO₂ (to suppress any bioreductive metabolism by endogenous one-electron reductases under hypoxia). Clonogenic survival of both populations was determined by plating in selective media containing ouabain or puromycin, and the concentration providing 10% survival (C₁₀) was estimated by interpolation. Values are mean ± SEM or range for the number of experiments shown in parentheses. ^b C₁₀ for activators in co-cultures. ^c C₁₀ for targets in co-cultures. ^d C₁₀ for targets in MCLs grown from target cells only. ^e A_C and T_C values reported in ref 10.

hydrophilic diol carboxamide side chains. This suggests that extravascular penetration of the prodrugs becomes less efficient at low logP values.

The magnitude of bystander effects was assessed by determining how effectively the presence of activator cells shifted the survival curve for target cells toward that of the activators themselves. A typical experiment, with the bromomesylate mustard **39**, is illustrated in Figure 2B. This shows that MCLs comprising 100% target cells have a C₁₀ greater than the solubility limit ($T > 250 \mu\text{M}$), while targets in MCL co-cultures are much more sensitive ($T_C = 10 \mu\text{M}$). The latter C₁₀ value was only 5-fold higher than that for the activators themselves ($A_C = 2 \mu\text{M}$) despite the activators representing only 2.1% of the cells in this group of MCLs.

The magnitude of the bystander effect for each compound was compared using the ratio A_C/T_C , which assumes a value of unity when the target cells become as sensitive as the activators in the co-cultures. Notably, for 18 of the 22 nitrogen mustards investigated, the A_C/T_C ratio was higher than for **1** ($A_C/T_C = 0.14$). As reported previously for a subset of the dichloromustards,¹⁰ there was a relationship between the magnitude of the bystander effect (A_C/T_C ratio) and logP of the prodrugs, as illustrated in Figure 2C. This presumably reflects an underlying correlation between the logP of prodrug and active metabolites, with more efficient transcellular diffusion of the more lipophilic reduction products. However, for this larger compound set it is possible to discern logP-independent effects of the leaving groups on bystander efficiency, as shown by progressive displacement of the A_C/T_C versus logP plots for the more-reactive dibromo- and diiodomustards (Figure 2C). This suggests a reduced diffusion range with increasing leaving group

reactivity (Cl < Br < I) at equivalent lipophilicity, as a result of reaction of the corresponding activated metabolites during diffusion.

The oxygen-linked leaving groups (mesylate and sulfamoylate) gave hydrophilic compounds with low bystander effects, although the mixed halomesylate mustards (**36**, **39**, and **43**, respectively) provided A_C/T_C values (0.16, 0.2, and 0.35, respectively) at least as high as **1**. The high NTR ratios of these three compounds in the IC₅₀ panel, coupled with their encouraging bystander effects, suggested that evaluation against NTR-expressing tumors should extend to these relatively hydrophilic analogs.

PLS-Based QSAR Analysis of MCL Data. PLS was also applied to fit the bystander efficiency (A_C/T_C ratios) for the 22 mustards in Table 2, using the same physicochemical descriptors as above. PLS modeling of the bystander efficiency (A_C/T_C ratio) resulted in two PCs ($R^2 = 86.8\%$ and $Q^2 = 68.5\%$; Model 4; Figure S2). The most influential parameters positively correlating with high bystander efficiency were the hydrophobicity (π) of the side chain and mustard leaving groups (LG1 > LG2) that contribute to overall lipophilicity, while size and hydrogen bonding ability of the side chain and steric factors of the leaving groups (LG1 > LG2) were negatively correlated (Table S3 and Figure S1). In addition, both the electronic and the nucleofugality parameters indicated that higher leaving group reactivity, particularly of the more-reactive one, resulted in lower bystander efficiency. This suggests that smaller, more lipophilic compounds give a better bystander effect due their increased ability to diffuse (i.e., to cross the lipid cell membrane), but that there are limits on the reactivity of the metabolites to ensure that they can efficiently reach the target cells.

Activity against NTR-Expressing Tumors. A diverse series of compounds (essentially the set investigated for transport in the MCL assay) was selected for evaluation in mice. These included representative dibromomustards and mixed mustards with high potency and selectivity for NTR-expressing cell lines, but also included compounds with lesser activity in vitro, such as chloromustards with solubilizing side chains and the morpholide **16**. The in vivo parameters, including maximum tolerated dose (MTD) and activity against NTR-expressing EMT6 and WiDr tumors in CD-1 nude mice, are summarized in Table 3.

MTDs were determined after single i.p. doses, mainly using formulations containing dimethylsulfoxide (DMSO) or dimethylacetamide (DMA)/polyethylene glycol 400 (PEG)/water mixtures. During the study it was found that the toxicity of some compounds was higher when administered in DMSO/PEG/water than in neat DMSO, as illustrated for **23** and **48** in Table 3. Despite this complicating factor, there were clearly large differences in toxicity within the series; even restricting the comparison to compounds tested in DMSO alone, there was a 10-fold range of MTD values. Several analogs with reactive bromo and/or mesylate leaving groups (e.g., the dibromo analogs **23** and **26** and bromomesylate **39**) were surprisingly well tolerated despite their high cytotoxic potency against NTR^{-ve} cell lines in vitro relative to the corresponding dichloromustards (Table 1).

The activity of these compounds was assessed at the MTD against NTR^{+ve} tumor cells using two assays. Killing of EMT6 NTR^{+ve} cells in mixed tumors comprising about 95% wild-type NTR^{-ve} EMT6 cells was determined by tumor excision and clonogenic assay 18 h after treatment. These experiments used puromycin in the plating medium to quantify the surviving NTR^{+ve} cells in the mixture; logarithms of cell kill (LCK) are

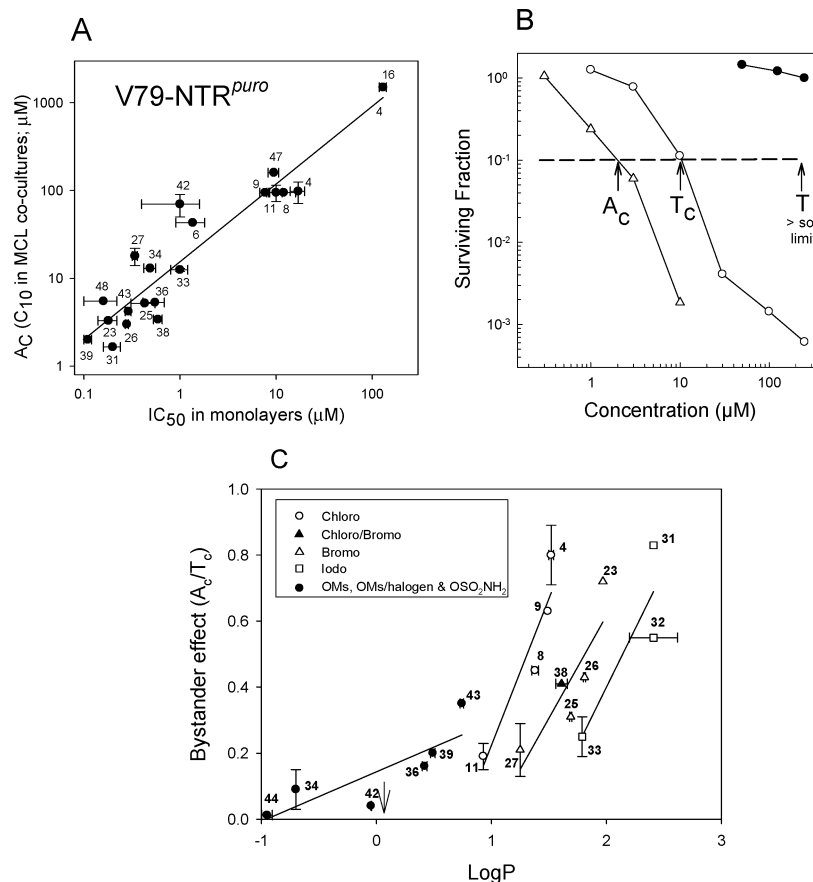


Figure 2. Cytotoxicity and bystander effects of 2,4-dinitrobenzamide-5-mustards in V79 MCL cultures comprising 3% V79-NTR^{puro} cells, following 5 h exposure to the prodrugs. MCLs were grown either from NTR-ve V79^{oua} target cells alone or mixtures of 3% NTR⁺ve V79-NTR^{puro} activator cells with 97% target cells. (A) Relationship between cytotoxicity against V79-NTR^{puro} cells in monolayer (IC₅₀, 18 h exposure) and in MCL co-cultures (C₁₀ for activators, A_c, 5 h exposure). Error bars are SEM or range for independent experiments, and the line is the linear regression. (B) A representative bystander effect experiment, with **39**. ●: 100% targets (C₁₀ value = T). △: activators in co-cultures (C₁₀ value = A_c). ○: targets in co-cultures (C₁₀ = T_c). (C) Relationship between logP of prodrugs and bystander effect in MCL (A_c/T_c ratio). Error bars are SEM for logP and the range of duplicate experiments for A_c/T_c (single determinations were not shown). Lines are linear regressions through the compound sets defined by the key (excluding the single mixed halogen mustard **38**). The arrow beside **42** indicates that the plotted value is an upper estimate.

reported in Table 3. Activity against tumors grown from WiDr-NTR^{neo} cells was assessed by measuring tumor volume changes after treatment; median tumor growth delay to reach an endpoint tumor size of 15 mm mean diameter are reported in Table 3 along with the numbers of long-term controls (tumors not palpable 100 days after treatment).

In the EMT6 assay, aziridine **1** or dichloromustard **4** was included as an internal standard in each experiment. Aziridine **1** showed significant activity in 5/5 experiments, with activity close to or above the sensitivity limit of approximately 3 logs of kill. The dichloromustard **4** appeared to be slightly less active, achieving statistical significance in 3/4 experiments with 1–3 logs of kill. For simplicity, only one representative experiment for **1** and **4** is shown in Table 3. The morpholide **16** was inactive, consistent with its weak activation by NTR in vitro, and most of the other dichloromustards had moderate activity (comparable to **4**). Very high activity was seen against EMT6-NTR^{puro} cells, beyond the dynamic range of the assay, with the dibromo compounds **23**, **26**, and **27**, the dimesylate **34**, and the mixed mustards **36**, **38**, and **39**. This subgroup of compounds with the highest in vivo activity displayed a combination of low IC₅₀ values against EMT6-NTR^{puro} cells (Table S2 in Supporting Information) and high MTD values. The ratio MTD/IC₅₀ appeared to be predictive of in vivo activity, with values >2370 μmol/kg/μM for all compounds in this highly active set (median

value 11,240), while for the set with lower in vivo activity (**4**, **6**, **8**, **9**, **11**, **16**, **31**, **33**, and **48**), this ratio ranged from 10 to 2500 (median 151).

In the WiDr-NTR^{neo} tumor growth delay assay, the aziridine (**1**) was used as a positive control in all experiments and consistently provided a high proportion of complete regressions of tumors comprising 100% NTR⁺ve cells. Over all experiments using **1** at a dose of 200 μmol/kg in 43 mice, 36 tumors were fully controlled at 100–120 days, while there were four deaths ascribed to drug toxicity. The 13 dinitrobenzamide mustards assayed against these tumors provided a wide range of activities; the morpholide **16** and diiodo derivatives **31** and **33** showed little or no activity, while seven compounds (**23**, **26**, **34**, **36**, **39**, **43**, and **48**) were highly active, with frequent long-term tumor control and median growth delays of >80 days. There was a strong concordance between the EMT6 and the WiDr tumor assays for the compounds assayed in both; these identified the same core set of compounds with high activity (**1**–**3**, **26**, **34**, **36**, **39**, and **48**) and the same inactive or marginally active compounds (**16** and **33**), while **4** and **11** had intermediate activity in both. Activity in the two models was discordant only for the diiodomustard **31**, which provided moderate and significant activity against EMT6-NTR^{puro} cells, but not against WiDr-NTR^{neo} tumors.

To compare the efficiency of the bystander effect resulting from activation by NTR, tumor growth inhibition and cure was

Table 3. MTDs and Antitumor Activity of 2,4-Dinitrobenzamide-5-mustards against NTR-Expressing Murine (EMT6) and Human (WiDr) Tumors

No	vehicle ^a	MTD ^b	EMT6 tumor excision assay ^c		WiDr tumor growth delay ^f					
			LCK ^d	<i>p</i> ^e	10% NTR ⁺ ve tumors			100% NTR ⁺ ve tumors		
					GD ^g	cures ^h	<i>p</i> ⁱ	GD	cures	<i>p</i> ⁱ
1	DMA/PEG ^j	200	3.16 ± 0.10	<0.05	14	0/6	<0.05	>88 ⁿ	3/6	<0.001
4	DMA/PEG	200	2.29 ± 0.18	<0.05	11	0/6	<0.01	29	2/7	<0.05
6	DMSO ^k	133	0.38 ± 0.09	NS ^p						
8	DMA/PEG	133	>2.02 ^o	<0.05						
9	DMSO/PEG ^l	178	0.44 ± 0.12	NS						
11	DMA/PEG	560	1.49 ± 0.34	<0.05				75	1/5	<0.001
16	Acetate ^m	300	0.07 ± 0.29	NS				27	1/6	<0.01
23	DMSO	>1330			20	2/7	<0.001	>84	6/7	<0.001
					21	1/7	<0.001			
	DMSO/PEG	562	4.17 ± 0.03	<0.05				>84	5/5	<0.01
26	DMSO	1780			7	1/9	NS			
					13	0/6	0.001			
	DMSO/PEG	562	>3.44	<0.05				>83	2/4	<0.001
27	DMSO/PEG	1330	>3.36	<0.05	22	1/5	<0.001			
31	DMA/PEG	200	1.48 ± 0.18	<0.05				8	0/5	NS
33	DMSO/PEG	237	0.54 ± 0.21	NS				37	0/3	<0.05
34	DMSO	2000	>2.60	<0.05	20	0/6	<0.001	>82	8/8	<0.001
36	DMSO	1000	>4.03	<0.05	38	1/7	<0.001	>80	3/3	<0.01
			>3.82	<0.05						
			>3.02	<0.05						
38	DMSO	237	>3.61	<0.05	26	1/8	<0.001	>82	6/6	<0.001
39	DMSO	1780			9	0/9	NS	55	2/7	<0.001
42	DMSO	1330			15	0/7	<0.001	>82	6/7	<0.001
43	DMSO	1330			36	1/8	<0.001	>83	2/5	<0.001
48	DMSO	750								
	DMSO/PEG	133	2.24 ± 0.24	<0.05						

^a Formulation for dosing mice. In all experiments animals received a single ip dose. ^b MTD in CD-1 nude mice ($\mu\text{mol/kg}$ body weight). ^c Determined 18 h after treatment of mice with mixed EMT6/EMT6-NTR^{neo} tumors (mean diameter 8.5–11.5 mm) at the MTD. ^d Log cell kill (LCK) = $\log \text{CS}_{\text{control}} - \log \text{CS}_{\text{treated}}$, where CS is the number of clonogenic survivors/g tumor. Values are mean \pm SEM for groups of 3–5 animals. ^e Probability that the difference from control is due to chance (ANOVA plus Dunnett's test). ^f WiDr tumors were grown by inoculating either 10% WiDr-NTR^{neo}/90% WiDr or 100% WiDr-NTR^{neo} cells and treating when tumors reached a mean diameter of 7.0–8.5 mm. ^g GD: median growth delay (days), including cures, determined as $\text{TTE}_{\text{treated}} - \text{TTE}_{\text{control}}$, where TTE is time to endpoint (15 mm mean tumor diameter). ^h Probability that the difference from vehicle-only control is due to chance (Log rank test). ⁱ Proportion of animals with controlled tumors at termination (100 days after treatment). ^j 10% dimethylacetamide/40% polyethylene glycol/50% water v/v/v, 10 $\mu\text{L/g}$ body weight. ^k 100% dimethylsulfoxide, 1 $\mu\text{L/g}$ body weight. ^l 10% dimethylsulfoxide/40% polyethylene glycol/50% water v/v/v, 10 $\mu\text{L/g}$ body weight. ^m 25 mM sodium acetate buffer, pH 4.0, 10 $\mu\text{L/g}$ body weight. ⁿ This group (with 3–7 animal) was included for quality control in all nine experiments; a representative experiment is shown. ^o > in this column indicates that no colonies were detected from at least one tumor in the group. The value is the mean for the remaining tumors. ^p NS = not significant.

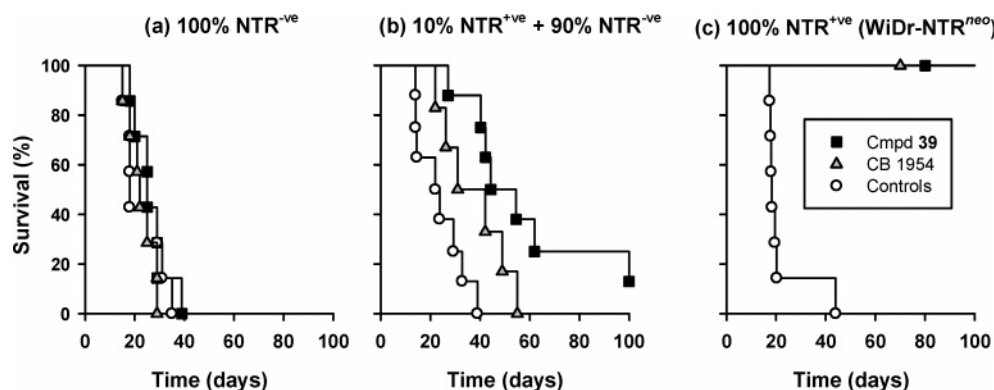


Figure 3. Kaplan–Meier survival curves for control of established (7–8.5 mm diameter) WiDr tumors by aziridine **1** and the dinitrobenzamide bromesylate mustard **39** following a single i.p. dose at its MTD (1780 $\mu\text{mol/kg}$). (A) Tumors grown from WiDr cells only (100% NTR^{-ve}). (B) Mixture of 10% WiDr-NTR^{neo} and 90% NTR^{-ve} WiDr cells. (C) WiDr-NTR^{neo} cells only. The ordinate shows the percentage of mice alive with tumors less than the endpoint size of 15 mm mean diameter.

also assessed using WiDr tumors grown from a mixture of 10% NTR⁺ve and 90% NTR^{-ve} cells (Table 3). In this case, tumor control was achieved much less frequently and median growth delays were greatly reduced, although statistically significant activity was observed with all compounds except the hydrophilic Br/OMs diol **42**, which also showed a very low bystander effect in V79 MCLs (Figure 1C; $A_C/T_C < 0.05$). Typical experiments comparing **1** and the more lipophilic Br/OMs mustard **39** (which had a greater bystander effect than **1** in the MCL assay) against WiDr tumors with varying proportions of NTR⁺ve cells are illustrated in Figure 3. Neither compound showed significant

activity against NTR^{-ve} WiDr tumors (Figure 3A) and both provided a high rate of long-term control of 100% NTR tumors (Figure 3C). Against tumors with 10% NTR⁺ve cells (Figure 3B), the increase in median survival time was 32 days for **39** versus 9 days for **1**. Log rank survival analysis demonstrated highly significant differences between the three curves ($p < 0.001$), and the Holm–Sidak multiple comparison test demonstrated that the difference between **39** and control was significant ($p < 0.05$) but that the activity of **1** was not. The 23-day difference in median growth delay between **39** and **1** was also significant ($p < 0.05$). Thus, we conclude that **39** has a greater

bystander effect than **1** in WiDr tumors containing 10% NTR⁺ cells.

Conclusions

This investigation of 2,4-dinitrobenzamide-5-mustards, including 32 new examples, as prodrugs for *E. coli* NTR (the *nsfB* gene product) demonstrates a broadly consistent SAR for cytotoxic activation across four genetic backgrounds (human WiDr colon carcinoma and Skov3 ovarian carcinoma, EMT6 mouse mammary carcinoma, and V79 chinese hamster fibroblasts). Analogs with reactive leaving groups (especially bromo and mesylate) show higher potencies and NTR selectivities than dichloromustards, with 15 of these compounds providing submicromolar IC₅₀ values; similar to or more potent than the aziridinyldinitrobenzamide (**1**). A range of carboxamide side chains (especially monoalcohols) are tolerated and can be used to increase aqueous solubility, although basic tertiary amine side chains suppress NTR selectivity in all cases and dihydroxy side chains lower potency when combined with mesylate leaving groups on the mustard moiety.

Multivariate regression analysis of the IC₅₀ results, using a PLS model, showed that in NTR^{-ve} lines cytotoxicity correlated negatively with H-bond donating/accepting groups but positively with logP and with the reactivity of the less-reactive mustard leaving group; the latter observation is consistent with cytotoxicity resulting from DNA monoadducts arising from a half-mustard that is formed through intramolecular alkylation by the more-reactive mustard arm. In contrast, in NTR⁺ lines the efficiency of the more-reactive leaving group is more important, reflecting DNA crosslinking ability. High NTR ratios correlated with high logP, small carboxamide side chains with low numbers of HA and high HD, and with asymmetric halomustards.

The above QSAR is that for an intact cellular system, and it is thus unlikely to depend only on the QSAR for NTR. It is notable that the dominant features of the cellular QSAR (high lipophilicity and low H-bond acceptor density) are those expected for passive diffusion across the plasma membrane. Thus, the overall QSAR may reflect rate-limiting membrane transport as much as the substrate specificity of NTR.

Bystander effects in three-dimensional MCL cultures (grown from mixtures of NTR⁺ and NTR^{-ve} cells) also correlated positively with logP, as did cytotoxic potency relative to low cell density cultures. The apparent loss of efficiency of penetration of the prodrugs, and intercellular diffusion of their metabolites, at low logP reflects the classical conflict in drug development between the need for lipophilicity for adequate membrane penetration and the hydrophilicity for aqueous solubility. In addition, bystander killing was suppressed by the reactive leaving groups that enhanced potency (bystander efficiency Cl > Br > I). Despite these constraints relative to the lipophilic dichloromustard **4**, which has a markedly superior bystander effect to **1**,^{7,10} 18/22 of the 2,4-dinitrobenzamide-5-mustards tested in the MCL assay provided equal or greater bystander killing than **1**. Given the central importance of the bystander effect for enzyme/prodrug systems in cancer therapy,²⁸ this commends the dinitrobenzamide mustards for further development as NTR prodrugs for GDEPT.

Surprisingly, the toxicity of the 2,4-dinitrobenzamide-5-mustards in mice was lower for the bromo-, mesylate- and bromomesylate mustards than for the less-reactive dichloromustards. This typically allowed administration of doses 5–10-fold higher than the dichloromustards or **1**. Consistent with this higher host tolerance and the higher potency against NTR-expressing cells in culture, the bromo-, mesylate- and bromome-

sylate compounds also showed the greatest activity against NTR⁺ cells in EMT6 and WiDr tumors. When the proportion of NTR⁺ cells in WiDr tumors was lowered by inoculation of 1:9 mixtures of NTR⁺ and NTR^{-ve} cells, antitumor activity was reduced but was still significant for most compounds. Under these conditions, where activity depends critically on a highly efficient bystander effect, the bromomesylate mustard **39** showed superior activity to **1**. This favorable therapeutic activity is consistent with its improvement over **1** in potency and NTR selectivity in the cell line panel in culture, its more efficient bystander effect in MCLs, and its higher MTD in mice. Despite its hydrophilic mesylate group, **39** is less water soluble than **1** or **4**. However, ongoing work suggests that key aspects of the SAR defined here carry over to a different dinitrobenzamide mustard regioisomer class, in which even higher NTR substrate efficiency and in vivo therapeutic activity can be achieved.

Experimental Section

Analyses were carried out in the Microchemical Laboratory, University of Otago, Dunedin, NZ. Melting points were determined on an Electrothermal 2300 melting point apparatus. NMR spectra were obtained on a Bruker DRX-400 spectrometer and are referenced to Me₄Si. Thin-layer chromatography was carried out on aluminum-backed silica gel (Merck 60 F₂₅₄) or alumina plates. Flash column chromatography was carried out on Merck silica gel (230–400 mesh) or alumina. Petroleum ether refers to the fraction boiling at 40–60 °C. Mass spectra were determined using a VG 7070 spectrometer.

5-[Bis(2-chloroethyl)amino]-N-hydroxy-2,4-dinitrobenzamide (6; Scheme 1). A solution of 5-[bis(2-chloroethyl)amino]-2,4-dinitrobenzoyl chloride (from acid **54**,¹⁶ 1.00 g, 2.70 mmol) in Et₂O (50 mL) was added in one portion to an ice-cold solution of hydroxylamine hydrochloride (0.75 g, 10.8 mmol) and Na₂CO₃ (1.18 g, 11.3 mmol) in water (10 mL). The mixture was shaken vigorously at room temperature for 5 min, then adjusted to pH 5 with 1 N aqueous HCl, and extracted with EtOAc. The extract was washed with 1 N aqueous HCl and satd aqueous NaCl, dried (Na₂SO₄), and evaporated. The residue was chromatographed on silica gel, eluting with EtOAc/CH₂Cl₂ (6:1), followed by crystallization from EtOAc/hexane, to give **6** (538 mg, 54%): mp 136–138 °C; ¹H NMR [(CD₃)₂SO] δ (mixture of rotamers) 11.18, 10.77 (2s, 1H), 9.39, 9.31 (2s, 1H), 8.58, 8.55 (2s, 1H), 7.44, 7.41 (2s, 1H), 3.82 (t, *J* = 5.9 Hz, 4H), 3.68 (t, *J* = 5.9 Hz, 4H). HRMS (FAB, *m/z*) calcd for C₁₁H₁₃³⁵Cl₂N₄O₆ (MH⁺), 367.02112; found, 367.0205. Anal. (C₁₁H₁₂Cl₂N₄O₆) C, H, N, Cl.

5-[Bis(2-chloroethyl)amino]-N-(2-hydroxyethoxy)-2,4-dinitrobenzamide (7). A stirred solution of *O*-(2-hydroxyethyl)-hydroxylamine (270 mg, 3.50 mmol) and diisopropylethylamine (184 mg, 1.42 mmol) in CH₂Cl₂ (20 mL) at 0 °C was treated dropwise with a solution of the acid chloride of **54** (526 mg, 1.42 mmol) in CH₂Cl₂ (10 mL). The mixture was stirred at room temperature for a further 15 min and then concentrated under reduced pressure. The residue was dissolved in EtOAc, washed with water, dried (Na₂SO₄), and evaporated, and the residue was chromatographed on silica gel. Elution with EtOAc, followed by concentration of the eluate to a small volume and dilution with *i*-Pr₂O, gave **7** (309 mg, 53%) as a gum; ¹H NMR [(CD₃)₂SO] δ (mixture of rotamers) 11.74 (br s, 1H), 8.61, 8.58 (2s, 1H), 7.62, 7.54 (2s, 1H), 4.74 (br s, 1H), 3.98 (t, *J* = 4.9 Hz, 2H), 3.82 (t, *J* = 5.9 Hz, 4H), 3.70 (t, *J* = 5.8 Hz, 4H), 3.67–3.62 (m, 2H). HRMS (FAB, *m/z*) calcd for C₁₃H₁₇³⁵Cl₂N₄O₇ (MH⁺), 411.0474; found, 411.0470.

N-(3-Hydroxypropyl)-5-[bis(2-chloroethyl)amino]-2,4-dinitrobenzamide (9). A solution of the acid chloride of **54** in Me₂CO (50 mL) at –5 °C was treated similarly with a cold solution of 3-amino-1-propanol (2 equiv) in water (25 mL). The reaction mixture was shaken at room temperature for 5 min, then diluted with water (25 mL), concentrated to half volume, and extracted

with CH_2Cl_2 (2 \times). The organic extract was washed with 0.1 N HCl and water and then worked up to give a solid that was chromatographed on silica gel, eluting with EtOAc to give **9** (2.37 g, 82%): mp (EtOAc/*i*-Pr₂O) 90–91 °C; ¹H NMR [(CD₃)₂SO] δ 8.63 (t, *J* = 5.6 Hz, 1H), 8.53 (s, 1H), 7.42 (s, 1H), 4.46 (t, *J* = 5.1 Hz, 1H), 3.82 (t, *J* = 5.9 Hz, 4H), 3.68 (t, *J* = 5.9 Hz, 4H), 3.49 (q, *J* = 6.0 Hz, 2H), 3.29 (q, partially obscured, *J* = 5.9 Hz, 2H), 1.68 (pent, *J* = 6.7 Hz, 2H). Anal. (C₁₄H₁₈Cl₂N₄O₆) C, H, N, Cl.

N-(2-Hydroxypropyl)-5-[bis(2-chloroethyl)amino]-2,4-dinitrobenzamide (10). Treatment of the acid chloride of **54** in Me₂CO with a solution of 1-amino-2-propanol (2.05 equiv) in water as above, followed by chromatography of the product on silica gel and elution with EtOAc, gave **10** (78% yield): mp (EtOAc/*i*-Pr₂O) 95–97 °C; ¹H NMR [(CD₃)₂SO] δ 8.70 (t, *J* = 5.8 Hz, 1H), 8.53 (s, 1H), 7.44 (s, 1H), 4.75 (d, *J* = 4.7 Hz, 1H), 3.86–3.75 (m, 5H), 3.68 (t, *J* = 5.9 Hz, 4H), 3.24–3.12 (m, 2H), 1.10 (d, *J* = 6.2 Hz, 3H). Anal. (C₁₄H₁₈Cl₂N₄O₆) C, H, N, Cl.

5-[Bis(2-chloroethyl)amino]-N-[2-hydroxy-1,1-bis(hydroxymethyl)ethyl]-2,4-dinitrobenzamide (12). A stirred, cooled suspension of the acid chloride of **54** (1.43 g, 3.86 mmol) in Me₂CO (30 mL) at 5 °C was treated with a solution of tris(hydroxymethyl)aminomethane (0.935 g, 7.72 mmol) in water (4 mL) in one portion, and the mixture was stirred with cooling for 15 min. The Me₂CO was removed under reduced pressure, and the residue was partitioned between EtOAc and 3 N HCl. The organic portion was worked up, and the residue was chromatographed on silica gel. Elution with EtOAc gave foreruns, followed by **12** (1.40 g, 80%): mp (EtOAc/petroleum ether) 168–171 °C; ¹H NMR [(CD₃)₂SO] δ 8.55 (s, 1H), 7.96 (br s, 1H), 7.52 (s, 1H), 4.56 (t, *J* = 6.0 Hz, 3H), 3.85 (t, *J* = 5.9 Hz, 4H), 3.72–3.33 (m, 10H). Anal. (C₁₅H₂₀Cl₂N₄O₈) C, H, N, Cl.

N-(2-Aminoethyl)-5-[bis(2-chloroethyl)amino]-2,4-dinitrobenzamide Hydrochloride (13). A suspension of *N*-(*t*-butyloxycarbonyl)ethylenediamine (0.21 g, 1.31 mmol) and Et₃N (0.25 mL, 1.78 mmol) in CH₂Cl₂ was added to a vigorously stirred solution of the acid chloride of **54** (0.44 g, 1.19 mmol) in CH₂Cl₂ (30 mL) at 0–5 °C. After stirring at room temperature for 15 min, the solution was washed with aqueous NaHCO₃ solution and worked up to give an oil, which was chromatographed on silica gel. Elution with EtOAc/petroleum ether (3:2) gave the crude BOC amide as a yellow gum that was immediately deprotected by dissolution in MeOH (20 mL) and concd HCl (5 mL). After standing at room temperature for 30 min, the solution was concentrated to dryness and evaporated to give the HCl salt of **13** (0.38 g, 72%): mp (MeOH/Et₂O) 115–118 °C (dec); ¹H NMR (D₂O) δ 8.84 (s, 1H), 7.59 (s, 1H), 3.86–3.79 (m, 8H), 3.76 (t, *J* = 6.2 Hz, 2H), 3.34 (t, *J* = 6.2 Hz, 2H). Anal. (C₁₃H₁₇Cl₂N₅O₅·HCl) C, H, N, Cl.

N-[3-(4-Morpholino)propyl]-5-[bis(2-chloroethyl)amino]-2,4-dinitrobenzamide (17). Treatment of the acid chloride of **54** with 4-(3-aminopropyl)morpholine (2.05 equiv) in cold CH₂Cl₂ as above, followed by chromatography of the product on silica gel and elution with EtOAc/MeOH (6:1), gave **17** (82%) as a gum; ¹H NMR [(CD₃)₂SO] δ 8.64 (t, *J* = 5.6 Hz, 1H), 8.54 (s, 1H), 7.42 (s, 1H), 3.82 (t, *J* = 5.9 Hz, 4H), 3.68 (t, *J* = 5.9 Hz, 4H), 3.57 (t, *J* = 4.6 Hz, 4H), 3.27 (q, partially obscured, *J* = 6.5 Hz, 2H), 2.40–2.28 (m, 6H), 1.68 (pent, *J* = 7.0 Hz, 2H). Treatment with EtOAc/petroleum ether/HCl gave the hydrochloride salt as a gum. Anal. (C₁₈H₂₅Cl₂N₅O₆·HCl) C, H, N, Cl.

N-[4-(4-Morpholino)butyl]-5-[bis(2-chloroethyl)amino]-2,4-dinitrobenzamide (18). Treatment of the acid chloride of **54** with 4-(4-aminobutyl)morpholine (2.05 equiv) in cold CH₂Cl₂ as above, followed by chromatography of the product on silica gel and elution with EtOAc/MeOH (9:1), gave **18** (74% yield) as an oil; ¹H NMR [(CD₃)₂SO] δ 8.64 (t, *J* = 5.6 Hz, 1H), 8.53 (s, 1H), 7.41 (s, 1H), 3.82 (t, *J* = 5.9 Hz, 4H), 3.68 (t, *J* = 5.9 Hz, 4H), 3.56 (t, *J* = 4.6 Hz, 4H), 3.24 (q, *J* = 6.1 Hz, 2H), 2.38–2.23 (m, 6H), 1.59–1.44 (m, 4H). Treatment with EtOAc/petroleum ether/HCl gave the hydrochloride salt, mp (MeOH/*i*-Pr₂O) 51–54 °C. Anal. (C₁₉H₂₇Cl₂N₅O₆·HCl) C, H, N, Cl.

N-[2-(Imidazol-1-yl)ethyl]-5-[bis(2-chloroethyl)amino]-2,4-dinitrobenzamide (19). Treatment of the acid chloride of **54** with 1-(2-aminoethyl)imidazole in cold CH₂Cl₂ as above, followed by multiple recrystallizations of the product from EtOAc, gave **19** (72% yield): mp 139–140 °C; ¹H NMR [(CD₃)₂SO] δ 8.84 (t, *J* = 5.7 Hz, 1H), 8.54 (s, 1H), 7.66 (s, 1H), 7.26 (s, 1H), 7.23 (s, 1H), 6.91 (s, 1H), 4.16 (t, *J* = 5.8 Hz, 2H), 3.83 (t, *J* = 5.9 Hz, 4H), 3.68 (t, *J* = 5.8 Hz, 4H), 3.56 (q, *J* = 5.8 Hz, 2H). Treatment with MeOH/EtOAc/petroleum ether/HCl gave the hydrochloride salt, mp (MeOH/*i*-Pr₂O) 83–86 °C. Anal. (C₁₆H₁₈Cl₂N₆O₅·HCl·0.5H₂O) C, H, N, Cl.

N-[3-(Imidazol-1-yl)propyl]-5-[bis(2-chloroethylamino)]-2,4-dinitrobenzamide (20). Treatment of the acid chloride of **54** with 1-(3-aminopropyl)imidazole in cold CH₂Cl₂ as above, followed by multiple recrystallizations of the product from EtOAc, gave **20** (77% yield): mp 142–143 °C; ¹H NMR [(CD₃)₂SO] δ 8.72 (t, *J* = 5.6 Hz, 1H), 8.56 (s, 1H), 7.64 (s, 1H, imidazole-H), 7.46 (s, 1H), 7.20 (d, *J* = 0.9 Hz, 1H), 6.91 (s, 1H), 4.06 (t, *J* = 6.9 Hz, 2H), 3.83 (t, *J* = 5.8 Hz, 4H), 3.69 (t, *J* = 5.8 Hz, 4H), 3.20 (q, *J* = 6.3 Hz, 2H), 2.00–1.90 (m, 2H). Treatment with MeOH/EtOAc/petroleum ether/HCl gave the hydrochloride salt as a gum. Anal. (C₁₇H₂₀Cl₂N₆O₅·HCl·0.5H₂O) C, H, N, Cl.

5-[Bis(2-chloroethyl)amino]-N-(methylsulfonyl)-2,4-dinitrobenzamide (22). A solution of methanesulfonamide (635 mg, 6.68 mmol) in dry DMF (10 mL) was treated at 0 °C with NaH (255 mg, 6.38 mmol, 60% in oil). The stirred mixture was warmed to room temperature for 1 h, then cooled to 0 °C, and added to an ice-cold solution of the acid chloride of **54** (1.18 g, 3.18 mmol) in dry CH₂Cl₂ (20 mL). The mixture was stirred at room temperature for 30 min, then diluted with CH₂Cl₂, washed with 0.1 N aqueous AcOH and saturated aqueous NaCl, dried (Na₂SO₄), and evaporated. Chromatography on silica gel, eluting with EtOAc, followed by crystallization from CH₂Cl₂, gave **22** (708 mg, 52%): mp 173–175 °C; ¹H NMR [(CD₃)₂SO] δ 12.51 (br s, 1H), 8.62 (s, 1H), 7.68 (s, 1H), 3.84 (t, *J* = 5.7 Hz, 4H), 3.72 (t, *J* = 5.7 Hz, 4H), 3.37 (s, 3H). Anal. (C₁₂H₁₄Cl₂N₄O₇) C, H, N, Cl.

5-[Bis(2-bromoethyl)amino]-N-hydroxy-2,4-dinitrobenzamide (24) and 5-[N-(2-Bromoethyl)-N-[2-[(methylsulfonyl)oxy]ethyl]amino]-2,4-dinitrobenzamide (40). A stirred solution of methyl 5-[bis(2-hydroxyethyl)amino]-2,4-dinitrobenzoate¹⁶ (**49**; 5.50 g, 16.7 mmol) and Et₃N (5.82 mL, 41.8 mmol) in dry CH₂Cl₂ (50 mL) was treated dropwise at 0 °C with MsCl (3.14 mL, 40.0 mmol). After 30 min, 10% aqueous KHCO₃ (100 mL) was added, and the mixture was stirred for a further 30 min at 0 °C and then diluted with petroleum ether (500 mL). The precipitated product was collected and washed with water and *i*-Pr₂O to give methyl 5-(bis{2-[(methylsulfonyl)oxy]ethyl}amino)-2,4-dinitrobenzoate (**50**; 7.44 g, 92%): mp (CH₂Cl₂/petroleum ether) 157–158 °C; ¹H NMR [(CD₃)₂SO] δ 8.62 (s, 1H), 7.77 (s, 1H), 4.35 (t, *J* = 5.1 Hz, 4H), 3.88 (s, 3H), 3.73 (t, *J* = 5.1 Hz, 4H), 3.13 (s, 6H). Anal. (C₁₄H₁₉N₂O₁₂S₂) C, H, N, S.

Hydrolysis of **50** (3.0 g, 6.18 mmol) with 3 N KOH (40 mL) in a mixture of dioxane (160 mL) and MeOH (40 mL) at room temperature for 15 min, followed by acidification with 1 N HCl and extraction with EtOAc, gave crude 5-(bis{2-[(methylsulfonyl)oxy]ethyl}amino)-2,4-dinitrobenzoic acid (**52**; 90%). The product, which contained polar impurities due to mustard group hydrolysis, was used for the next step without further purification; ¹H NMR [(CD₃)₂SO] δ 14.1 (v br s, 1H), 8.57 (s, 1H), 7.69 (s, 1H), 4.34 (t, *J* = 5.1 Hz, 4H), 3.72 (t, *J* = 5.1 Hz, 4H), 3.13 (s, 6H).

A suspension of **52** (1.28 g, 2.72 mmol) in SOCl₂ (30 mL) containing DMF (2 drops) was heated under reflux for 1 h. Evaporation of the solvent under reduced pressure, followed by azeotroping with benzene, gave the crude acid chloride. This was dissolved in EtOAc (50 mL), and the solution was diluted with Et₂O (25 mL) and treated at 0 °C in one portion with a solution of hydroxylamine hydrochloride (0.75 g, 10.8 mmol) and Na₂CO₃ (0.86 g, 8.11 mmol) in water (10 mL). The mixture was shaken at room temperature for 15 min and then diluted with water. The organic phase was washed with water (3 \times), dried, and concentrated under reduced pressure. The residue was chromatographed on silica

gel, eluting with EtOAc/MeOH (24:1), and the eluate was concentrated to a small volume and diluted with hexane to precipitate 5-[bis[2-[(methylsulfonyl)oxy]ethyl]amino]-*N*-hydroxy-2,4-dinitrobenzamide (**53**; 0.94 g, 71%) as an unstable yellow gum, which was used directly: $^1\text{H NMR}$ [(CD₃)₂SO] δ (mixture of rotamers) 11.18, 10.79 (2s, 1H), 9.40, 9.32 (2s, 1H), 8.59, 8.56 (2s, 1H), 7.48, 7.46 (2s, 1H), 4.34 (t, $J = 5.1$ Hz, 4H), 3.71 (t, $J = 5.0$ Hz, 4H), 3.13, 3.12 (2s, 6H).

A mixture of **53** (940 mg, 1.93 mmol) and LiBr (201 mg, 2.31 mmol) in MeCN (30 mL) was stirred at reflux for 45 min and then concentrated under reduced pressure. The residue was chromatographed on silica gel, eluting with EtOAc/CH₂Cl₂ (11:9), and the eluate was concentrated to a small volume and diluted with hexane to give **24** (320 mg, 36%) as a yellow gum: $^1\text{H NMR}$ [(CD₃)₂SO] δ (mixture of rotamers) 11.20, 10.77 (2s, 1H), 9.40, 9.31 (2s, 1H), 8.58, 8.55 (2s, 1H), 7.42, 7.39 (2s, 1H), 3.79–3.64 (m, 8H). HRMS (FAB, m/z) calcd for C₁₁H₁₃⁷⁹Br₂N₄O₆ (MH⁺), 454.9202; found, 454.9167.

Further elution with EtOAc, followed by concentration to a small volume and dilution with hexane, gave **40** (188 mg, 21%) as a yellow gum: $^1\text{H NMR}$ [(CD₃)₂SO] δ (mixture of rotamers) 11.18, 10.78 (2s, 1H), 9.40, 9.31 (2s, 1H), 8.59, 8.55 (2s, 1H), 7.45, 7.43 (2s, 1H), 4.33 (t, $J = 5.1$ Hz, 2H), 3.77–3.64 (m, 6H), 3.13, 3.12 (2s, 3H). HRMS (FAB, m/z) calcd for C₁₂H₁₆⁷⁹BrN₄O₉S (MH⁺), 470.9821; found, 470.9832.

***N*-(2-Hydroxyethyl)-5-[bis(2-bromoethyl)amino]-2,4-dinitrobenzamide (25)**. A solution of ester **50** (2.50 g, 5.15 mmol) in EtOAc (200 mL) was treated with LiBr (10.0 g, 115 mmol) at 55 °C for 30 min. The reaction mixture was poured into water (100 mL), and the organic layer was washed with water, dried, and evaporated under reduced pressure to give methyl 5-[*N,N*-bis(2-bromoethyl)amino]-2,4-dinitrobenzoate (**51**; 2.20 g, 94%) as a yellow solid: mp (EtOAc/petroleum ether) 168–170 °C; $^1\text{H NMR}$ [(CD₃)₂SO] δ 8.61 (s, 1H), 7.77 (s, 1H), 3.89 (s, 3H), 3.76 (t, $J = 5.8$ Hz, 4H), 3.68 (t, $J = 5.8$ Hz, 4H). Anal. (C₁₂H₁₃Br₂N₃O₆) C, H, N.

A solution of **51** (2.29 g 5.03 mmol) in 1,4-dioxane (60 mL) was treated at 5 °C with a solution of KOH (9.0 g) in water (20 mL), followed by MeOH (20 mL). The reaction mixture was stirred at room temperature for 15 min and then acidified with 1 N HBr and extracted with EtOAc (3 × 100 mL). The combined organic layers were dried and evaporated to give 5-[bis(2-bromoethyl)amino]-2,4-dinitrobenzoic acid (**55**) as a yellow solid: mp (MeOH/water, followed by EtOAc/*i*-Pr₂O/petroleum ether) 132–134 °C; $^1\text{H NMR}$ [(CD₃)₂SO] δ 14.0 (br, 1H), 8.56 (s, 1H), 7.66 (s, 1H), 3.75 (t, $J = 6.1$ Hz, 4H), 3.65 (t, $J = 6.0$ Hz, 4H). Anal. (C₁₁H₁₁-Br₂N₃O₆) C, H, N.

A suspension of powdered **55** (1.10 g, 2.49 mmol) in benzene (230 mL) was treated at 10 °C with oxalyl chloride (1.10 mL, 12.6 mmol) and DMF (2 drops). The mixture was stirred at 10 °C for 3 h, then concentrated under reduced pressure below 25 °C, and re-evaporated to dryness in the presence of benzene. The resulting acid chloride was dissolved in Me₂CO (20 mL), and the solution was treated at –5 °C with a cold solution of 2-aminoethanol (0.30 g, 5.19 mmol) in water (10 mL). The mixture was shaken at room temperature for 5 min, then diluted with water, and extracted with EtOAc (2×). The organic extract was worked up, and the resulting residue was chromatographed on silica gel, eluting with EtOAc, to give **25** (0.78 g, 46%): mp (MeOH/EtOAc/petroleum ether) 151–152 °C; $^1\text{H NMR}$ [(CD₃)₂SO] δ 8.73 (t, $J = 5.7$ Hz, 1H), 8.53 (s, 1H), 7.43 (s, 1H), 4.76 (t, $J = 5.6$ Hz, 1H), 3.77–3.64 (m, 8H), 3.53 (q, $J = 6.0$ Hz, 2H), 3.31 (q, partially obscured, $J = 6.1$ Hz, 2H). Anal. (C₁₃H₁₆Br₂N₄O₆) C, H, N, Br.

***N*-(3-Hydroxypropyl)-5-[bis(2-bromoethyl)amino]-2,4-dinitrobenzamide (26)**. Similar reaction of the acid chloride of **55** with 3-amino-1-propanol gave **26** (1.06 g, 85%): mp (EtOAc/*i*-Pr₂O) 85–86 °C; $^1\text{H NMR}$ [(CD₃)₂SO] δ 8.64 (t, $J = 5.6$ Hz, 1H), 8.53 (s, 1H), 7.41 (s, 1H), 3.77–3.64 (m, 8H), 4.46 (br s, 1H), 3.49 (t, $J = 6.3$ Hz, 2H), 3.33–3.25 (m, partially obscured, 2H), 1.68 (pent, $J = 6.7$ Hz, 2H). Anal. (C₁₄H₁₈Br₂N₄O₆) C, H, N, Br.

***N*-(2,3-Dihydroxypropyl)-5-[bis(2-bromoethyl)amino]-2,4-dinitrobenzamide (27)**. Similar treatment of the acid chloride of

55 with a solution of 3-amino-1,2-propanediol, followed by chromatography on silica gel, eluting with EtOAc, gave **27** (2.2 g, 83%) as a foam; $^1\text{H NMR}$ [(CD₃)₂SO] δ 8.71 (t, $J = 5.8$ Hz, 1H, CONH), 8.53 (s, 1H, H-3), 7.43 (s, 1H, H-6), 4.86 (d, $J = 5.0$ Hz, 1H, CHOH), 4.59 (t, $J = 5.8$ Hz, 1H, CH₂OH), 3.70–3.10 (m, 13H); $^{13}\text{C NMR}$ δ 164.61, 146.65, 137.99, 137.35, 136.52, 124.25, 121.20, 70.05, 63.73, 52.44, 42.76, 30.33. HRMS (FAB, m/z) calcd for C₁₄H₁₉⁷⁹Br₂N₄O₇ (MH⁺), 512.9621; found, 512.9596.

***N*-[3-(4-Morpholino)propyl]-5-[bis(2-bromoethyl)amino]-2,4-dinitrobenzamide (29)**. Treatment of the acid chloride of **55** with 4-(3-aminopropyl)morpholine in cold CH₂Cl₂, as previously described, followed by chromatography of the product on silica gel and elution with EtOAc/MeOH (4:1) gave **29** (82% yield) as a foam: $^1\text{H NMR}$ [(CD₃)₂SO] δ 8.65 (t, $J = 5.6$ Hz, 1H), 8.54 (s, 1H, H-3), 7.40 (s, 1H), 3.78–3.64 (m, 8H), 3.57 (t, $J = 4.6$ Hz, 4H), 3.32–3.22 (m, 2H), 2.40–2.30 (m, 6H), 1.68 (pent, $J = 7.0$ Hz, 2H). Anal. (C₁₈H₂₅Br₂N₅O₆) C, H, N, Br.

Methyl 3-({5-[Bis(2-bromoethyl)amino]-2,4-dinitrobenzoyl}-amino)propanoate (28; Scheme 2). A solution of 5-chloro-2,4-dinitrobenzoic acid (**56**; 10.0 g, 40 mmol) in SOCl₂ (100 mL) containing DMF (2 drops) was heated under reflux for 5 h and concentrated to dryness. Residual reagent was removed by the addition of benzene, followed by concentration to dryness again. A solution of the resulting crude acid chloride in ether (30 mL) was added at 0 °C to a vigorously stirred solution of methyl 3-aminopropanoate [prepared by dissolving the hydrochloride (6.22 g, 44 mmol) in water (20 mL), then diluting with Me₂CO (100 mL) and Et₂O (100 mL), and neutralizing with Et₃N (13.0 mL, 0.10 mol)]. The mixture was stirred for 30 min, and the resulting precipitate was filtered off, washed well with water, and recrystallized from EtOAc/petroleum ether to give methyl 3-[(5-chloro-2,4-dinitrobenzoyl)amino]propanoate (**57**; 6.24 g, 47%): mp 139–141 °C; $^1\text{H NMR}$ [(CD₃)₂SO] δ 8.98 (t, $J = 5.6$ Hz, 1H), 8.83 (s, 1H), 8.09 (s, 1H), 3.63 (s, 3H), 3.47 (dt, $J = 6.7, 5.6$ Hz, 2H), 2.61 (t, $J = 6.7$ Hz, 2H); $^{13}\text{C NMR}$ δ 171.49 (CO₂CH₃), 162.71 (CONH), 147.13 (s), 144.89 (s), 135.97 (s), 132.33 (d), 130.42 (s), 122.12 (d), 51.40 (CO₂CH₃), 35.18 (t), 32.83 (t).

A solution of **57** (4.0 g, 12 mmol) and diethanolamine (2.53 g, 24 mmol) in dioxane (100 mL) and MeOH (20 mL) was stirred at room temperature for 18 h and then concentrated to dryness under reduced pressure. The residue was partitioned between EtOAc and water, and the organic portion was worked up to give an oil that was chromatographed on silica gel. Elution with MeOH/EtOAc (1:19) gave methyl 3-({5-[bis(2-hydroxyethyl)amino]-2,4-dinitrobenzoyl}amino)propanoate (**58**; 4.28 g, 87%) as an orange oil: $^1\text{H NMR}$ [(CD₃)₂SO] δ 8.72 (t, $J = 5.6$ Hz, 1H), 8.47 (s, 1H), 7.28 (s, 1H), 4.80 (t, $J = 5.3$ Hz, 2H), 3.62 (s, 3H), 3.57 (dd, $J = 5.8, 5.3$ Hz, 4H), 3.46 (dd, $J = 6.8, 5.6$ Hz, 2H), 3.42 (t, $J = 5.8$ Hz, 4H), 2.60 (t, $J = 6.8$ Hz, 2H); $^{13}\text{C NMR}$ δ 171.58 (CO₂CH₃), 165.01 (CONH), 147.74 (s), 136.94 (s), 136.13 (s), 133.66 (s), 124.61 (d), 119.50 (d), 58.04 (CH₂OH), 54.10 (CH₂N), 51.37 (CO₂CH₃), 35.07 (CH₂COHN), 30.62 (CH₂CO₂CH₃). MS [M + H]⁺ calcd for C₁₅H₂₀N₄O₉, 401.1308; found, 401.1300 (CI mass spectrum).

Methanesulfonyl chloride (1.72 mL, 22 mmol) was added dropwise at 0 °C to a solution of **58** (3.89 g, 9.70 mmol) and Et₃N (3.38 mL, 24 mmol) in CH₂Cl₂ (100 mL). After 15 min, the solution was washed with saturated aqueous NaHCO₃ (3×) and water (2×). After drying over Na₂SO₄, the solution was concentrated to about 20 mL, and the product was precipitated out by the addition of petroleum ether (50 mL). A mixture of the resulting crude dimesylate and LiBr (10 g) in EtOAc (200 mL) was warmed at 50–55 °C for 30 min and then concentrated to dryness. The residue was partitioned between EtOAc and water, and the organic portion was worked up to give an oil that was chromatographed on silica gel. Elution with EtOAc/petroleum ether (1:1) gave **28** (3.50 g, 68%) as a yellow oil: $^1\text{H NMR}$ [(CD₃)₂SO] δ 8.82 (t, $J = 5.6$ Hz, 1H), 8.54 (s, 1H), 7.39 (s, 1H), 3.73, 3.69 (2 × br t, $J = 5.7$ Hz, 8H), 3.47 (dt, $J = 6.7, 5.6$ Hz, 2H), 3.34 (s, 3H), 2.62 (t, $J = 6.7$ Hz, 2H); $^{13}\text{C NMR}$ δ 171.60 (CO₂CH₃), 164.46 (CONH), 146.69 (s), 137.84 (s), 137.10 (s), 136.12 (s), 124.35 (d), 120.79 (d), 52.46 (CO₂CH₃), 51.39 (CH₂N), 35.09 (CH₂CONH), 32.90 (CH₂CO₂CH₃),

30.31 (CH₂Br). MS M⁺ calcd for C₁₅H₁₈Br₂N₄O₇, 527.9501, 525.9522, 523.9542; found, 527.9502, 525.9535, 523.9545.

3-(5-(Bis(2-bromoethyl)amino)-2,4-dinitrobenzamido)propanoic Acid (30). A solution of **28** (4.00 g, 7.58 mmol) and 1 N NaOH (20 mL, 20 mmol) in 1:1 THF/MeOH (80 mL) was stirred at room temperature for 2 h. After acidification with 3 N HBr, the solution was concentrated to a small volume and extracted with EtOAc. Workup gave **30** (3.11 g, 80%): mp (Me₂CO/water) 166 °C; ¹H NMR [(CD₃)₂SO] δ 12.29 (br, 1H), 8.79 (t, *J* = 5.6 Hz, 1H), 8.54 (s, 1H), 7.40 (s, 1H), 3.73, 3.68 (2 × br t, *J* = 5.1 Hz, 8H), 3.43 (dt, *J* = 6.9 Hz, 2H), 2.53 (t, *J* = 6.9, 5.6 Hz, 2H); ¹³C NMR δ 172.70 (CO₂H), 164.43 (CONH), 146.67 (s), 137.86 (s), 137.18 (s), 136.16 (s), 124.31 (d), 120.84 (d), 52.36 (CH₂N), 35.16 (CH₂CONH), 33.13 (CH₂CO₂CH₃), 30.33 (CH₂Br). Anal. (C₁₄H₁₆Br₂N₄O₇·0.5Me₂CO) C, H.

N-(2-Hydroxyethyl)-5-[bis(2-bromoethyl)amino]-2,4-dinitrobenzamide (25) and 2-((2-Bromoethyl)-5-[(2-hydroxyethyl)amino]carbonyl)-2,4-dinitroanilinoethyl Methanesulfonate (41; Scheme 3). A solution of the acid chloride of **52** (3.20 g, 6.79 mmol) in dry Me₂CO (80 mL) was treated at 0 °C with 2-aminoethanol (1.24 g, 20.3 mmol). After stirring at 0 °C for 5 min, the mixture was acidified to pH 2–3 with 0.2 N HBr, concentrated to half volume, and then solid NaBr was added. The mixture was extracted with EtOAc (2 ×), and the combined extracts were washed with saturated NaBr solution, dried (Na₂SO₄), and evaporated. The residue was chromatographed on silica gel, eluting with EtOAc/MeOH (15:1), to give 2-(5-[(2-hydroxyethyl)amino]carbonyl){2-[(methylsulfonyloxy)ethyl]-2,4-dinitroanilino}ethyl methanesulfonate (**60**; 2.87 g, 82%) as a gum that was used directly.

A mixture of **60** (1.80 g, 3.50 mmol) and LiBr (0.43 g, 4.95 mmol) in DMF (5 mL) was stirred at 60 °C for 2 h. The reaction was then poured into a saturated NaBr solution and extracted with EtOAc (2 ×). The combined extracts were washed with saturated NaBr solution, dried (Na₂SO₄), and concentrated under reduced pressure. The residue was chromatographed on silica gel, eluting with EtOAc, to give **25** (0.78 g, 46%).

Further elution with EtOAc/MeOH (9:1) gave **41** (0.73 g, 42%): mp (EtOAc) 102–104 °C; ¹H NMR [(CD₃)₂SO] δ 8.70 (t, *J* = 5.7 Hz, 1H), 8.54 (s, 1H), 7.46 (s, 1H, H-6), 4.76 (*J* = 5.5 Hz, 1H), 4.34 (t, *J* = 5.1 Hz, 2H), 3.74 (t, *J* = 5.1 Hz, 2H), 3.70 (br s, 4H), 3.53 (q, *J* = 6.0 Hz, 2H), 3.31 (q, partially obscured, *J* = 6.1 Hz, 2H), 3.14 (s, 3H). Anal. (C₁₄H₁₉BrN₄O₉S·0.25EtOAc; detected by NMR) C, H, N.

5-[Bis(2-iodoethyl)amino]-N-(2-hydroxyethyl)-2,4-dinitrobenzamide (32). A stirred mixture of **60** (1.42 g, 2.76 mmol) and NaI (3.3 g, 22 mmol) in dry MeCN (45 mL) was heated at reflux for 1 h and then concentrated under reduced pressure. The residue was partitioned between EtOAc and water, and the organic layer was washed with water and evaporated. The residue was chromatographed on silica gel, eluting with CH₂Cl₂/EtOAc (1:4), followed by recrystallization from MeOH/EtOAc/*i*-Pr₂O to give **32** (2.9 g, 81%): mp 142–143 °C; ¹H NMR [(CD₃)₂SO] δ 8.73 (t, *J* = 5.7 Hz, 1H), 8.53 (s, 1H), 7.38 (s, 1H), 4.76 (t, *J* = 5.5 Hz, 1H), 3.68 (t, *J* = 6.9 Hz, 4H), 3.57–3.49 (m, 2H), 3.39 (t, *J* = 6.9 Hz, 4H), 3.34–3.26 (m, partially obscured, 2H). Anal. (C₁₂H₁₆I₂N₄O₆) C, H, N, I.

2-(5-[(2,3-Dihydroxypropyl)amino]carbonyl){2-[(methylsulfonyloxy)ethyl]-2,4-dinitroanilino}ethyl Methanesulfonate (35) and 2-((2-Chloroethyl)-5-[(2,3-dihydroxypropyl)amino]carbonyl)-2,4-dinitroanilinoethyl Methanesulfonate (37). The acid chloride of **52** (2.9 g, 6.18 mmol; containing some of the corresponding chloromethylate) was treated with 3-amino-1,2-propanediol for 10 min, then acidified to pH 2–3 with 1 N HCl. Most of the solvent was evaporated, and the residue was partitioned between water and EtOAc. The aqueous layer was extracted with EtOAc (2 × 80 mL), and the combined organic phases were dried and evaporated under reduced pressure. The residue was adsorbed directly onto silica gel and chromatographed. Elution with EtOAc gave 2-((2-chloroethyl)-5-[(2,3-dihydroxypropyl)amino]carbonyl)-2,4-dinitroanilinoethyl methanesulfonate **37** (0.5 g, 17%) as a yellow solid: mp 118–121 °C (EtOAc); ¹H NMR [(CD₃)₂SO] δ

8.68 (t, *J* = 3.3 Hz, 1H), 8.53 (s, 1H), 7.46 (s, 1H), 4.82 (d, *J* = 5.0 Hz, 1H), 4.56 (t, *J* = 5.7 Hz, 1H), 4.33 (t, *J* = 5.1 Hz, 2H), 3.83 (t, *J* = 6.1 Hz, 2H), 3.73 (t, *J* = 5.1 Hz, 2H), 3.64 (m, 3H), 3.44–3.38 (m, 4H), 3.13 (s, 3H); ¹³C NMR δ 164.51, 147.08, 138.03, 137.30, 136.45, 124.20, 121.38, 70.01, 66.74, 63.68, 52.92, 49.68, 42.70, 41.54, 36.56. Anal. (C₁₅H₂₁ClN₄O₁₀S) C, H, N.

Further elution with EtOAc/MeOH (from 50:1 to 10:1) gave **35** (2.38 g, 71%) as a yellow oil: ¹H NMR [(CD₃)₂SO] δ 8.66 (t, *J* = 5.8 Hz, 1H, CONH), 8.54 (s, 1H, H-3), 7.48 (s, 1H, H-6), 4.81 (d, *J* = 5.0 Hz, 1H, CHOH), 4.59 (t, *J* = 5.1 Hz, 1H, CH₂OH), 4.35 (m, 4H, 2 × CH₂OMs), 3.66 (m, 4H), 3.62 (m, 1H), 3.46–3.36 (m, 4H), 3.13 (s, 6H); ¹³C NMR δ 164.48, 147.09, 138.26, 137.27, 136.60, 124.17, 121.72, 70.02, 66.69 (2), 63.68, 50.21 (2), 42.68, 36.55 (2). HRMS (FAB, *m/z*) calcd for C₁₆H₂₅N₄O₁₃S₂, 545.0860 (MH⁺); found, 545.0856.

2-((2-Bromoethyl)-5-[(2,3-dihydroxypropyl)amino]carbonyl)-2,4-dinitroanilinoethyl Methanesulfonate (42). A solution of **35** (1.28 g, 2.53 mmol) in EtOAc (100 mL) was treated with LiBr (347 mg, 4.0 mmol) at 60 °C for 2 h. Volatiles were removed under reduced pressure, and the residue was adsorbed directly onto silica gel and chromatographed. Elution with EtOAc gave 5-[bis(2-bromoethyl)amino]-N-(2,3-dihydroxypropyl)-2,4-dinitrobenzamide (**27**; 0.4 g 31%). Further elution with EtOAc/MeOH (from 1:0 to 5:1) gave **42** (0.62 g, 46%): mp (EtOAc) 117–118 °C; ¹H NMR [(CD₃)₂SO] δ 8.68 (t, *J* = 5.8 Hz, 1H), 8.53 (s, 1H), 7.46 (s, 1H), 4.82 (d, *J* = 5.0 Hz, 1H), 4.56 (t, *J* = 5.1 Hz, 1H), 4.32 (m, 2H), 3.75–3.60 (m, 7H), 3.46–3.36 (m, 4H), 3.13 (s, 3H); ¹³C NMR δ 164.48, 146.84, 138.05, 137.29, 136.52, 124.18, 121.40, 70.01, 66.74, 63.68, 52.89, 49.56, 42.69, 36.55, 30.20. Anal. (C₁₅H₂₁BrN₄O₁₀S) C, H, N, Br.

5-[(2-Bromoethyl)(2-chloroethyl)amino]-2,4-dinitrobenzamide (38; Scheme 4). A mixture of 5-[(2-chloroethyl){2-(methylsulfonyloxy)ethyl}amino]-2,4-dinitrobenzamide¹⁶ (**36**; 0.91 g, 2.2 mmol) and LiBr (0.21 g, 2.4 mmol) in anhydrous MeCN (25 mL) was stirred under reflux for 1.5 h and then concentrated under reduced pressure. The residue was chromatographed on silica gel, eluting with CH₂Cl₂/EtOAc (3:2) to give a crude product contaminated with the dibromomustard **23**. Purification by multiple recrystallization from EtOAc/*i*-Pr₂O gave **38** (595 mg, 68%): mp 153 °C; ¹H NMR [(CD₃)₂SO] δ 8.52 (s, 1H), 8.17–7.82 (2 × s, 2H), 7.43 (s, 1H, H-6), 3.82 (t, *J* = 5.8 Hz, 2H), 3.77–3.63 (m, 6H). Anal. (C₁₁H₁₂BrClN₄O₅) C, H, N, Cl.

5-[(2-Bromoethyl){2-(methylsulfonyloxy)ethyl}amino]-2,4-dinitrobenzamide (39). A mixture of 5-[bis-[(2-methylsulfonyloxy)ethyl]amino]-2,4-dinitrobenzamide¹⁶ (**34**; 1.60 g, 3.4 mmol) and LiBr (356 mg, 4.1 mmol) in anhydrous MeCN (30 mL) was stirred under reflux for 1 h. The mixture was concentrated under reduced pressure, and the residue was chromatographed on silica gel. Elution with EtOAc/CH₂Cl₂ (11:9) gave the dibromomustard **23**, while further elution with EtOAc/CH₂Cl₂ (3:1) gave **39** (0.61 g, 39%): mp (EtOAc/*i*-Pr₂O) 160–161 °C; ¹H NMR [(CD₃)₂SO] δ 8.53 (s, 1H, H-3), 8.14, 7.83 (2 × s, 2H), 7.46 (s, 1H, H-6), 4.33 (t, *J* = 5.1 Hz, 2H), 3.74 (t, *J* = 5.1 Hz, 2H, NCH₂), 3.70 (br s, 4H), 3.14 (s, 3H). Anal. (C₁₂H₁₅BrN₄O₈S) C, H, N, Br.

5-[N-(2-Iodoethyl)-N-[2-(methylsulfonyloxy)ethyl]amino]-2,4-dinitrobenzamide (43). A mixture of **34** (1.12 g, 2.38 mmol) and NaI (0.46 g, 3.07 mmol) in anhydrous MeCN (20 mL) was stirred at reflux for 1 h. The mixture was concentrated under reduced pressure, and the residue was chromatographed on silica gel. Elution with EtOAc/CH₂Cl₂ (1:1) gave the diiodomustard, while further elution with EtOAc/CH₂Cl₂ (3:1) gave **43** (0.49 g, 41%): mp (Me₂CO/EtOAc/*i*-Pr₂O) 160 °C; ¹H NMR [(CD₃)₂SO] δ 8.52 (s, 1H, H-3), 8.14–7.83 (2 × s, 2H), 7.44 (s, 1H, H-6), 4.33 (t, *J* = 5.1 Hz, 2H), 3.73 (t, *J* = 5.1 Hz, 2H), 3.65 (t, *J* = 6.9 Hz, 2H), 3.40 (t, *J* = 6.9 Hz, 2H), 3.13 (s, 3H). Anal. (C₁₂H₁₅I₂N₄O₈S) H, N, I, C; found 29.4; calculated 28.7%.

2,2'-(5-Carbamoyl-2,4-dinitrophenylazanediyl)bis(ethane-2,1-diyl) Disulfamate (44). A solution of 5-[bis(2-hydroxyethyl)amino]-2,4-dinitrobenzamide¹⁶ (**61**; 300 mg, 0.95 mmol) in DMA (3 mL) was treated at –5 °C with sulfamoyl chloride (441 mg, 3.82 mmol). The mixture was stirred at 0 °C for 15 min and at room temperature

for 1 h and then partitioned between EtOAc and saturated aqueous NaCl. The organic phase was washed with saturated aqueous NaCl, dried (Na₂SO₄), and evaporated. The residue was crystallized from EtOAc/CH₂Cl₂ and then MeOH/EtOAc/hexane to give **44** (324 mg, 72%): mp 143–144 °C (dec); ¹H NMR [(CD₃)₂SO] δ 8.53 (s, 1H), 8.06, 7.85 (2s, 2H), 7.53 (s, 4H), 7.47 (s, 1H), 4.18 (t, *J* = 5.2 Hz, 4H), 3.67 (t, *J* = 5.2 Hz, 4H). Anal. (C₁₁H₁₆N₆O₁₁S₂) C, H, N, C: found 28.6; calculated 28.0%.

5-[Bis(2-chloroethyl)amino]-2-(methylsulfonyl)-4-nitrobenzamide (45; Scheme 5). A mixture of 5-chloro-2-methylsulfonyl-4-nitrobenzamide⁷ (**62**; 0.66 g, 2.37 mmol), bis(2-chloroethyl)amine hydrochloride (1.27 g, 7.11 mmol), and *i*-Pr₂NEt (0.98 g, 7.58 mmol) in anhydrous dioxane (25 mL) was stirred at 60 °C for 48 h. Additional bis(2-chloroethyl)amine hydrochloride (0.63 g, 3.53 mmol) and *i*-Pr₂NEt (0.46 g, 3.56 mmol) were then added, and the mixture was stirred at 60 °C for a further 36 h. Addition of water precipitated a yellow solid that was chromatographed on silica gel, eluting with EtOAc/CH₂Cl₂ (3:1) to give **45** (0.69 g, 76%): mp (EtOAc) 189–190 °C; ¹H NMR [(CD₃)₂SO] δ 8.24 (s, 1H), 8.20, 7.82 (2 × s, 2H), 7.43 (s, 1H), 3.82 (t, *J* = 6.1 Hz, 4H), 3.66 (t, *J* = 6.1 Hz), 3.40 (s, 3H). Anal. (C₁₂H₁₅Cl₂N₃O₅S) C, H, N, Cl.

***N*-(2,3-Dihydroxypropyl)-5-[bis(2-chloroethyl)amino]-2-(methylsulfonyl)-4-nitrobenzamide (46).** A suspension of 5-chloro-2-methylsulfonyl-4-nitrobenzoic acid⁷ (**63**; 2.21 g, 7.9 mmol) in SOCl₂ (20 mL) containing DMF (2 drops) was heated under reflux for 1 h, then concentrated under reduced pressure, and re-evaporated with benzene. The resulting acid chloride was dissolved in Me₂CO (40 mL), and the solution was treated at –5 °C with a cold solution of 3-amino-1,2-propanediol (1.51 g, 16.6 mmol) in water (20 mL). The mixture was shaken at room temperature until homogeneous, diluted with water (20 mL), concentrated under reduced pressure to 20 mL, and then extracted with EtOAc (3×). The organic extract was worked up, and the crude product was chromatographed on silica gel, eluting with EtOAc, to give *N*-(2,3-dihydroxypropyl)-5-chloro-2-methylsulfonyl-4-nitrobenzamide (**64**; 2.46 g, 88%): mp (EtOAc/*i*-Pr₂O) 141–142 °C; ¹H NMR [(CD₃)₂SO] δ 8.83 (t, *J* = 5.7 Hz, 1H), 8.55 (s, 1H), 8.08 (s, 1H, H-6), 4.81 (d, *J* = 5.0 Hz, 1H), 4.55 (t, *J* = 5.8 Hz, 1H), 3.70–3.60 (m, 1H), 3.45 (s, 3H), 3.44–3.35 (m, 3H), 3.17–3.06 (m, 1H). Anal. (C₁₁H₁₃ClN₂O₇S) C, H, N.

Benzamide **64** was reacted with bis(2-chloroethyl)amine hydrochloride under the conditions described for **45**. The reaction mixture was further heated at 60 °C for 2 h in the presence of *N,N*-dimethylethylenediamine (0.5 equiv) to quench the unreacted chloro derivative (which had similar chromatographic mobility to the desired product on TLC). The mixture was then concentrated under reduced pressure, and the residue was shaken with 0.5 N AcOH. The resulting solution was saturated with NaCl, extracted with EtOAc (2×), and worked up. The crude product was chromatographed on silica gel, eluting with EtOAc/MeOH (19:1), to give **46** (57% yield) as a gum: ¹H NMR [(CD₃)₂SO] δ 8.71 (t, *J* = 5.8 Hz, 1H), 8.24 (s, 1H), 7.46 (s, 1H), 4.74 (d, *J* = 4.8 Hz, 1H), 4.52 (t, *J* = 5.8 Hz, 1H), 3.82 (t, *J* = 6.0 Hz, 4H), 3.70–3.61 (m, partially obscured, 1H), 3.66 (t, *J* = 5.9 Hz, 4H), 3.45–3.36 (m, 3H), 3.40 (s, 3H), 3.17–3.06 (m, 1H). Anal. (C₁₃H₂₁Cl₂N₃O₇S·0.5EtOAc) C, H, N.

5-[Bis(2-bromoethyl)amino]-4-methylsulfonyl-2-nitrobenzamide (48). A mixture of recrystallized (MeOH/EtOAc) 5-[bis(methylsulfonyl)ethyl]amino-4-methylsulfonyl-2-nitrobenzamide²³ (**65**; 0.70 g, 1.39 mmol) and LiBr (0.72 g, 8.29 mmol) in DMF (10 mL) was stirred at 60 °C for 2 h and then concentrated under reduced pressure below 60 °C. The resulting solid was purified by chromatography on silica gel, eluting with EtOAc/CH₂Cl₂ (2:1), to give **48** (0.54 g, 82%): mp (EtOAc) 176–177 °C; ¹H NMR [(CD₃)₂SO] δ 8.49 (s, 1H), 8.22–7.90 (2 × s, 2H), 7.72 (s, 1H, H-6), 3.76 (t, *J* = 7.1 Hz, 4H), 3.63 (t, *J* = 7.0 Hz, 4H), 3.49 (s, 3H). Anal. (C₁₂H₁₅Br₂N₃O₅S) C, H, N, Br, S.

Growth Inhibition (IC₅₀) Assays. All in vitro studies used aliquots of frozen solutions of compounds in DMSO, with a maximum DMSO concentration in culture of ≤0.5%. Compounds were evaluated for cytotoxicity (measured as IC₅₀ values following

an 18 h drug exposure) in four pairs of stably NTR-transfected mammalian cell lines and their NTR^{-ve} counterparts. The chinese hamster fibroblast NTR^{-ve} line (V79^{puro}) is a V79/4 chinese hamster fibroblast transfected with an empty shuttle vector, while the NTR^{+ve} line (V79-NTR^{puro}) is the corresponding NTR transfectant. These lines were originally named T78-1 and T79-A3, respectively.²¹ WiDr-NTR^{neo} (originally named WC14) is an NTR transfectant of the human colon carcinoma cell line WiDr. Skov3-NTR^{neo} (originally named SC3) is a transfectant of the human ovarian carcinoma line Skov3,²⁹ and EMT6-NTR^{puro} is from the murine breast carcinoma EMT6.²⁷ Cells were passaged in Alpha minimal essential medium (MEM) with 5% fetal calf serum (FCS; Gibco, Invitrogen Corporation) and G418 (0.3 mg/mL for WiDr-NTR^{neo}, 0.6 mg/mL for Skov3-NTR^{neo}) or puromycin (15 μM for V79^{puro} and V79-NTR^{puro}, 5 μM for EMT6-NTR^{puro}). IC₅₀ assays were performed as previously by sulforhodamine B (SRB) staining three (rodent cells) or four (human cells) days after washing out the prodrugs.¹⁵ IC₅₀ values were determined as the drug concentration for 50% inhibition of SRB staining relative to controls on the same 96-well plate. Selective cytotoxicity for NTR^{+ve} cells was assessed from the intra-experiment ratio of NTR^{-ve}/NTR^{+ve} IC₅₀ for each cell line pair.

MCL Assays for Bystander Effect. V79 MCLs were grown on collagen-coated Teflon microporous membranes as described previously^{10,27} by seeding with 10⁶ NTR^{-ve} V79^{oua} cells and 3 × 10⁴ (3% of total) V79-NTR^{puro} cells. The origin of the ouabain-resistant V79^{oua} cells has been reported previously.¹⁰ MCLs were grown submerged in stirred Alpha MEM with 5% FCS for 3 days and then exposed to prodrugs in 10 mL of the same medium with magnetic stirring under a 95% O₂/5% CO₂ gas phase (to reoxygenate the hypoxic center of MCLs and thus suppress any endogenous activation by one-electron reductases). MCLs were then trypsinised and centrifuged, and single cells were plated in nonselective medium (to measure total clonogens) or selective medium (1 mM ouabain to quantify surviving V79^{oua} cells and 15 μM puromycin to quantify surviving V79-NTR^{puro} cells). Surviving fractions for each population was calculated as the plating efficiency for drug-treated MCLs/plating efficiency for untreated controls.

Animals, Dosing, and Determination of Toxicity and Antitumor Activity. All animal experiments were performed under approvals from the University of Auckland Animal Ethics Committee. Specific pathogen free mice of either sex were used, with body weights of 20–30 g. Mice were housed in a temperature-controlled room with a 12-hour light/dark cycle. Drugs were administered as single ip doses using the vehicles and volumes indicated in Table 3. Toxicity was first evaluated in dose-ranging studies using C3H/HeN mice to establish the MTD, defined as the highest dose that did not cause death or body weight loss >15% or severe morbidity in any of six animals. This dose was used to treat CD-1 homozygous nude mice bearing dorsal subcutaneous EMT6 or WiDr tumors, which were grown by injecting a 2:1 mixture of EMT6-NTR^{puro}: EMT6 cells (total 3 × 10⁶ cells) or 10⁷ WiDr-NTR^{neo} cells (100% NTR^{+ve} WiDr tumors) or a mixture of 10⁶ WiDr-NTR^{neo} cells and 9 × 10⁶ WiDr cells (10% NTR^{+ve} WiDr tumors). Mice were ear-tagged and randomized to treatment groups (3–5 mice/group for EMT6, usually 5–7 mice/group for WiDr) without recaging when tumor diameters reached 8.5–11.5 mm (EMT6) or 7.0–8.5 mm mean diameter (WiDr tumors). EMT6 tumors were removed 18 h after drug treatment, dissociated with Pronase/collagenase/DNAase I, and plated in AlphaMEM with 5% FCS with or without 3 μM puromycin to assess clonogenic survival of NTR^{+ve} and total cells, respectively, as detailed previously.²⁷ Response of WiDr tumors was assessed by measuring orthogonal tumor diameters with callipers three times per week until endpoint (death, mean tumor diameter >15 mm, or 100 days after treatment). With rare exceptions, tumors were not palpable in animals surviving 100 days, and these were classed as cures. Median growth delay was determined, including cures in the analysis, and the statistical significance of drug effects were evaluated using the log rank test to make pairwise comparisons between treated and control groups.³

QSAR Modeling. PLS was performed using the package SIMCA-P 10.5 (Umetrics AB, Umeå, Sweden). The number of significant PCs was determined by seven internal cross validation rounds (i.e., leave ca. 14% out each time), and the fraction of explained variation (R^2 or “goodness of fit”) and the fraction of predicted variation of Y (Q^2 or “goodness of prediction”) were calculated. All PLS models were also validated by random permutation (100 times) of the Y values, and separate models were fitted to these permuted Y values by extracting the same number of PCs as was done in the original model. A plot of the correlation coefficients between the original and permuted Y values against R^2 and Q^2 gives a measure of over fitting. None of the PLS models were over fitted according to this validation method (not shown). In SIMCA-P a correction factor is applied to missing data (observations and/or variables) using a modified NIPALS algorithm to estimate a PC. IC_{50} values, NTR ratios, and bystander efficiencies were log-transformed in SIMCA-P. All X and Y variables were centered and scaled to unit variance. Hammett sigma constants for the mustard leaving groups were block scaled by $\sqrt[4]{K}$, where K is the number of variables in the block (12). Moderate outliers can be found in SIMCA by calculation of the observation distance to the model in the X space (DModX) and in the Y space (DModY), which are to X and Y residual standard deviations, respectively. No variable selection or pruning was attempted.

Physico-Chemical Descriptors. LogP_{7.4} (distribution coefficient in octanol/water at pH 7.4) and logP_{neutral} (partition coefficient in octanol/water of the neutral species) for the whole molecule were calculated using the program ACD/LogP v9.0 (Advanced Chemistry Development Labs, Inc., Ontario, Canada) using a combination of ACD/LogP System Training and Accuracy Extender. HA-side chain and HD-side chain are the number of hydrogen bond acceptors and donors in the side chain as determined by ACD/LogP (number of Ns and Os, and number of NHs and OHs, respectively). Sigma(Ind), Sigma(Res), Sigma(meta), Sigma(para), Sigma(Res-), and Sigma(Res+) are electronic substituent parameters, as calculated by ACD/Sigma, and refer to Sigma inductive, Sigma resonance (π -electron delocalization; benzoic acid model), Sigma meta for substituent in the meta-position on an aromatic ring (derived from benzoic acids), Sigma para for substituent in the para-position on an aromatic ring (derived from benzoic acids), Sigma aniline resonance (π -electron delocalization, aniline model), and Sigma plus resonance (π -electron delocalization from *t*-cumyl chlorides), respectively. MR (cm³), MV (cm³), Pi (Hansch hydrophobic constant π), MW (molecular weight), MA_p- K_a (most acidic p K_a), and MB_p- K_a (most basic p K_a) were calculated using ACD/LogP and ACD/p K_a . A prefix (LG1 or LG2) refers to the mustard leaving groups; no prefix refers to the whole side chain. The nucleofugality parameter ω (the postfix indicates LG1 or LG2), which describes the leaving group (LG) ability of the mustard leaving groups, was obtained from Jaramillo et al.,²⁴ who developed this scale in a CH₃LG model system.

Acknowledgment. This study was funded by Grant 01/276 from the Health Research Council of New Zealand. We thank Sarah Liyanage and Dr. Kevin Hicks for the determination of octanol/water partition coefficients.

Supporting Information Available: Growth inhibitory activity (IC_{50} values) for all eight cell lines investigated, and intra-experiment IC_{50} ratios, elemental analyses for all new compounds, and examples of PLS score and loading plots. This material is available free of charge via the Internet at <http://pubs.acs.org>.

References

- Denny, W. A.; Wilson, W. R. Consideration for the design of nitrophenyl mustards as agents with selective toxicity for hypoxic tumor cells. *J. Med. Chem.* **1986**, *29*, 879–887.
- Siim, B. G.; Denny, W. A.; Wilson, W. R. Nitro reduction as an electronic switch for bioreductive drug activation. *Oncol. Res.* **1997**, *9*, 357–369.
- Michael, N. P.; Brehm, J. K.; Anlezark, G. M.; Minton, N. P. Physical characterization of the *Escherichia coli* B gene encoding nitroreductase and its over-expression in *Escherichia coli* K12. *Microbiol. Lett.* **1994**, *124*, 195–202.
- Grove, J. I.; Searle, P. F.; Weedon, S. J.; Green, N. K.; McNeish, I. A.; Kerr, D. J. Virus-directed enzyme prodrug therapy using CB1954. *Anti-Cancer Drug Des.* **1999**, *14*, 461–472.
- Green, N. K.; Kerr, D. J.; Mautner, V.; Harris, P. A.; Searle, P. F. The nitroreductase/CB1954 enzyme-prodrug system. *Methods Mol. Med.* **2004**, *90*, 459–477.
- Knox, R. J.; Friedlos, F.; Marchbank, T.; Roberts, J. J. Bioactivation of CB 1954: Reaction of the active 4-hydroxylamino derivative with thioesters to form the ultimate DNA–DNA interstrand crosslinking species. *Biochem. Pharmacol.* **1991**, *42*, 1691–1697.
- Helsby, N. A.; Ferry, D. M.; Patterson, A. V.; Pullen, S. M.; Wilson, W. R. 2-amino metabolites are key mediators of CB 1954 and SN 23862 bystander effects in nitroreductase GDEPT. *Br. J. Cancer* **2004**, *90*, 1084–1093.
- Bridgewater, J. A.; Knox, R. J.; Pitts, J. D.; Collins, M. K.; Springer, C. J. The bystander effect of the nitroreductase/CB1954 enzyme/prodrug system is due to a cell-permeable metabolite. *Hum. Gene Ther.* **1997**, *8*, 709–717.
- Djeha, A. H.; Hulme, A.; Dexter, M. T.; Mountain, A.; Young, L. S.; Searle, P. F.; Kerr, D. J.; Wrighton, C. J. Expression of *Escherichia coli* B nitroreductase in established human tumor xenografts in mice results in potent antitumoral and bystander effects upon systemic administration of the prodrug CB1954. *Cancer Gene Ther.* **2000**, *7*, 721–731.
- Wilson, W. R.; Pullen, S. M.; Hogg, A.; Helsby, N. A.; Hicks, K. O.; Denny, W. A. Quantitation of bystander effects in nitroreductase suicide gene therapy using three-dimensional cell cultures. *Cancer Res.* **2002**, *62*, 1425–1432.
- Chung-Faye, G.; Palmer, D.; Anderson, D.; Clark, J.; Downes, M.; Baddeley, J.; Hussain, S.; Murray, P. I.; Searle, P.; Seymour, L.; Harris, P. A.; Ferry, D.; Kerr, D. J. Virus-directed, enzyme prodrug therapy with nitroimidazole reductase: A phase I and pharmacokinetic study of its prodrug, CB1954. *Clin. Cancer Res.* **2001**, *7*, 2662–2668.
- Bridgewater, J. A.; Springer, C. J.; Knox, R. J.; Minton, N. P.; Michael, N. P.; Collins, M. K. Expression of the bacterial nitroreductase enzyme in mammalian cells renders them selectively sensitive to killing by the prodrug CB1954. *Eur. J. Cancer* **1995**, *31A*, 2362–2370.
- Tang, M. H.; Helsby, N. A.; Wilson, W. R.; Tingle, M. D. Aerobic 2- and 4-nitroreduction of CB 1954 by human liver. *Toxicology* **2005**, *216*, 129–139.
- Anlezark, G. M.; Melton, R. G.; Sherwood, R. F.; Coles, B.; Friedlos, F.; Knox, R. J. The bioactivation of 5-(aziridin-1-yl)-2,4-dinitrobenzamide (CB1954) - I. Purification and properties of a nitroreductase enzyme from *Escherichia coli*—a potential enzyme for antibody-directed enzyme prodrug therapy (ADEPT). *Biochem. Pharmacol.* **1992**, *44*, 2289–2295.
- Helsby, N. A.; Atwell, G. J.; Yang, S.; Palmer, B. D.; Anderson, R. F.; Pullen, S. M.; Ferry, D. M.; Hogg, A.; Wilson, W. R.; Denny, W. A. Aziridinyl dinitrobenzamides: Synthesis and structure–activity relationships for activation by *E. coli* nitroreductase. *J. Med. Chem.* **2004**, *47*, 3295–3307.
- Palmer, B. D.; Wilson, W. R.; Atwell, G. J.; Schultz, D.; Xu, X. Z.; Denny, W. A. Hypoxia-selective antitumor agents. 9. Structure–activity relationships for hypoxia-selective cytotoxicity among analogues of 5-[*N,N*-bis(2-chloroethyl)amino]-2,4-dinitrobenzamide. *J. Med. Chem.* **1994**, *37*, 2175–2184.
- Anlezark, G. M.; Melton, R. G.; Sherwood, R. F.; Wilson, W. R.; Denny, W. A.; Palmer, B. D.; Knox, R. J.; Friedlos, F.; Williams, A. Bioactivation of dinitrobenzamide mustards by an *E. coli* B nitroreductase. *Biochem. Pharmacol.* **1995**, *50*, 609–618.
- Palmer, B. D.; van Zijl, P.; Denny, W. A.; Wilson, W. R. Reductive chemistry of the novel hypoxia-selective cytotoxin 5-[*N,N*-bis(2-chloroethyl)amino]-2,4-dinitrobenzamide. *J. Med. Chem.* **1995**, *38*, 1229–1241.
- Helsby, N. A.; Wheeler, S. J.; Pruijn, F. B.; Palmer, B. D.; Yang, S.; Denny, W. A.; Wilson, W. R. Effect of nitroreduction on the alkylating reactivity and cytotoxicity of the 2,4-dinitrobenzamide-5-aziridine CB 1954 and the corresponding nitrogen mustard SN 23862: Distinct mechanisms of bioreductive activation. *Chem. Res. Toxicol.* **2003**, *16*, 469–478.
- Johansson, E.; Parkinson, G.; Denny, W. A.; Neidle, S. Studies on the nitroreductase prodrug-activating system. Crystal structures of complexes with the inhibitor dicoumarol and dinitrobenzamide prodrugs and of the enzyme active form. *J. Med. Chem.* **2003**, *46*, 4009–4020.

- (21) Friedlos, F.; Denny, W. A.; Palmer, B. D.; Springer, C. J. Mustard prodrugs for activation by *Escherichia coli* nitroreductase in gene-directed enzyme prodrug therapy. *J. Med. Chem.* **1997**, *40*, 1270–1275.
- (22) Siim, B. G.; Hicks, K. O.; Pullen, S. M.; van Zijl, P. L.; Denny, W. A.; Wilson, W. R. Comparison of aromatic and tertiary amine *N*-oxides of acridine DNA intercalators as bioreductive drugs. Cytotoxicity, DNA binding, cellular uptake, and metabolism. *Biochem. Pharmacol.* **2000**, *60*, 969–978.
- (23) Atwell, G. J.; Boyd, M.; Palmer, B. D.; Anderson, R. F.; Pullen, S. M.; Wilson, W. R.; Denny, W. A. Synthesis and evaluation of 4-substituted analogues of 5-[*N,N*-bis(2-chloroethyl)amino]-2-nitrobenzamide as bioreductively activated prodrugs using an *Escherichia coli* nitroreductase. *Anti-Cancer Drug Des.* **1996**, *11*, 553–567.
- (24) Jaramillo, P.; Domingo, L. R.; Perez, P. Towards an intrinsic nucleofugality scale: The leaving group (LG) ability in CH3LG model system. *Chem. Phys. Lett.* **2006**, *420*, 95–99.
- (25) Wilson, W. R.; Hicks, K. O.; Pullen, S. M.; Ferry, D. M.; Helsby, N. A.; Patterson, A. V. Bystander effects of bioreductive drugs: potential for exploiting tumor hypoxia with dinitrobenzamide mustards. *Rad. Res.* **2007**, in press.
- (26) Kestell, P.; Pruijn, F. B.; Siim, B. G.; Palmer, B. D.; Wilson, W. R. Pharmacokinetics and metabolism of the nitrogen mustard bioreductive drug 5-[*N,N*-bis(2-chloroethyl)amino]-2,4-dinitrobenzamide (SN 23862) and the corresponding aziridine (CB 1954) in KHT tumour-bearing mice. *Cancer Chemother. Pharmacol.* **2000**, *46*, 365–374.
- (27) Wilson, W. R.; Pullen, S. M.; Hogg, A.; Hobbs, S. M.; Pruijn, F. B.; Hicks, K. O. In vitro and in vivo models for evaluation of GDEPT: Quantifying bystander killing in cell cultures and tumors. In *Suicide Gene Therapy: Methods and Reviews*; Springer, C. J., Ed.; Humana Press: Totowa, 2003; pp 403–432.
- (28) Patterson, A. V.; Saunders, M. P.; Greco, O. Prodrugs in genetic chemoradiotherapy. *Curr. Pharm. Des.* **2003**, *9*, 2131–2154.
- (29) Friedlos, F.; Court, S.; Ford, M.; Denny, W. A.; Springer, C. Gene-directed enzyme prodrug therapy: Quantitative bystander cytotoxicity and DNA damage induced by CB1954 in cells expressing bacterial nitroreductase. *Gene Ther.* **1998**, *5*, 105–112.

JM061062O